



PISTON ENGINE INTAKE AND EXHAUST SYSTEM DESIGN

P. O. A. L. DAVIES

*Institute of Sound and Vibration Research, University of Southampton,
Southampton SO17 1BJ, England*

(Received 1 July 1994, and in final form 21 March 1995)

The aim of intake and exhaust system design is to control the transfer of acoustic energy from the sources and its emission by the system with minimal loss of engine performance. A rational design process depends on the adoption of a design methodology based on predictive modelling of acoustic behaviour. Virtually any system geometry can be modelled by breaking it down to a sequence of simple elements or chambers. An initial design layout is then produced with simple parametric models of individual element behaviour. This design is then refined to prototype level by systematic modification of detail using realistic assessments of system performance in its operational environment. Following prototype validation by practical testing any further necessary development is again assisted by predictive modelling. The application of appropriate procedures is illustrated by a series of practical examples. These concern improvements in interior noise by control of intake noise, of vehicle performance by reducing flow losses, of the environment by control of exhaust emissions and lastly with the control of flow noise. This account concludes with a brief outline of current and new developments involving integrated hybrid design procedures. A further paper is being prepared describing silencer designs with their experimental validation.

©1996 Academic Press Limited

1. INTRODUCTION

The primary functions of an intake or exhaust system are firstly to efficiently channel fresh air to the engine and exhaust gas to the atmosphere, and secondly to minimize intake and exhaust noise emissions. Intakes must also filter particulates from the air while exhaust systems may be required to process the exhaust gas to satisfy prescribed exhaust emission standards or recover waste heat. Generally speaking, the gas must do work to reduce noise, which results in pressure loss and thus reduces flow efficiency, with a corresponding loss of engine performance. Therefore effective intake and exhaust system design involves finding the best compromise between minimizing noise emission and maximizing engine output and fuel efficiency.

There are a number of current initiatives concerned with the development of more realistic methods for improved intake and exhaust system design. Applications include road vehicles, tractors and commercial plant, rail traction, ship propulsion, power generation, etc. The objectives include more effective silencing performance to meet increasingly severe legislative targets for reduced noise and pollutant emissions on the one hand, with optimized engine performance and fuel economy accompanied by improvements in vehicle or plant subjective quality on the other. A typical procedure followed during the design and development of an exhaust system for a heavy truck is set out in Figure 1.

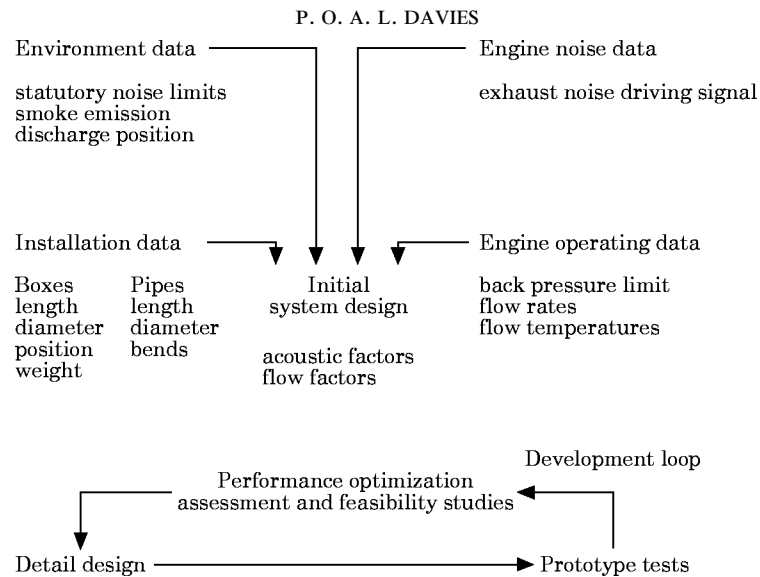


Figure 1. Muffler development scheme.

The design process includes a careful tuning of all components of the intake/exhaust system that influence noise emission with optimized matching of these to the engine operational and breathing characteristics that influence pollutant emissions, performance and economy. Together, these objectives can involve conflicting requirements, implying that integrated design procedures are strongly desirable, if not essential. Starting with an existing or notational system layout, an integrated assessment of the various performance aspects begins with a detailed evaluation of the cyclic wave action throughout the intake, valves, cylinder and exhaust corresponding to all likely conditions of engine operation [1]. This information may then be processed appropriately to assess current system performance in terms of the various design objectives, to provide a rational basis for systematic optimization of the design by implementing appropriate modifications to its constituent elements.

Aerodynamic processes associated with the cyclic flow through valves together with flow separation and vortex generation at junctions, expansions and the like provide the significant sources of inlet and exhaust noise through transfers of flow energy to wave energy. The acoustic characteristics of the corresponding intake and exhaust ducts have a direct influence on the extent and efficiency of such energy transfer [2], as well as controlling sound propagation along the ducts and sound emissions from their open terminations. Thus one finds that intake or exhaust noise emission can be controlled or modified by incorporating appropriate acoustically related geometrical and other features, either to minimize the energy transfer from sources or to attenuate the sound as it propagates through the system. This provides a fundamental base for intake/exhaust system design methodology.

The spectral characteristics of the exhaust signal are normally dominated by an extensive sequence of discrete tones that are harmonically related to the engine firing frequency. In many instances the bulk of the acoustic energy from the primary source is distributed among the lower frequency components that may be difficult to control. Significant intake noise emission is sometimes restricted to the first two or three such harmonics. Both practical experience and acoustic theory suggest that the spectral content of the acoustic

emissions of both intake and exhaust systems is strongly controlled by their acoustic characteristics: that is, their spectral behaviour as an acoustic filter, which is readily evaluated in the frequency domain. The noise emissions are also scaled in amplitude by the cyclic flow through the valves that provides the primary sources, which clearly are best evaluated in the time domain. However, since such engine operations are cyclic, the valve flow time histories can be subsequently Fourier analyzed to provide the corresponding spectral representation. Furthermore, noise emission measurements with the associated subjective and legislative assessments are normally performed in the frequency domain, and described in terms of the relevant spectral characteristics. Similar descriptions will be adopted in the discussion of acoustic behaviour presented here.

One notes that an alternative description, commonly adopted during vehicle development, is to classify the observed sound emissions into a sequence of harmonic orders of the engine rotational frequency, each member covering the whole range of operating speed at either full or part load. Such descriptions remain specific to each particular engine configuration: for example, with a four-cylinder four-stroke engine the significant orders are the second, fourth and so on and, although related to it, do not necessarily directly represent the overall acoustic performance of the intake or exhaust system.

The intake/exhaust system design process begins with the adoption of an appropriate methodology or design strategy. There are a number of alternative approaches, but all must take due account of the fact that the individual system elements, such as manifolds, pipes, junctions, silencing elements and the like all interact acoustically [3, 4]. Thus changes in the detail of one element may modify the combined acoustic behaviour of the remainder, and in particular, the acoustic characteristics of any sources that excite the system. See for example, Appendix C.

1.1. INTAKE/EXHAUST SYSTEM DESIGN STRATEGY

The primary aim of intake and exhaust system acoustic design is to minimize both the acoustic power transfer from the source and then its transmission along the system to the open termination where it is radiated. This forms the major consideration in what follows herein. However, depending on the application, other factors have a direct influence on the design of each individual system, together with the appropriate procedures for its realization. These include space, geometrical and operational constraints, unit cost, reliability, durability and complexity, subjective reaction to emitted spectral characteristics (noise quality) etc. Of this list, the influence of space constraints on acoustic design options always requires consideration, due to the practical restrictions it imposes.

In the past, successful silencer system design and development has been largely empirical, guided by a wealth of practical experience. A common situation concerns an existing engine with its intake and exhaust system which has either been uprated or installed in a new vehicle, resulting in the need for a systematic sequence of design changes, or modifications of detail, to meet noise emission standards. However, such an approach is often expensive in terms of manpower, time and other resources since each modified system must be fabricated and tested before its performance can be assessed. With a new engine or design project this “cut and try” approach to acoustic design can be tedious and prohibitively expensive, while lacking a corresponding level of confidence that an optimum or even a satisfactory result will be achieved.

Such considerations have led to the development of more rationally based acoustic design strategies where validated acoustic modelling [3–5] guided by insight and experience is harnessed to the computing power of modern desk top computers to refine an existing design or develop a new one. As summarized in Table 1 it consists of five basic steps, the

TABLE 1

Rational silencer design procedures

<i>Step I</i>	<i>Assemble relevant data</i> (i) existing noise signature (ii) required noise levels etc. (iii) installation physical and geometric constraints (iv) gas inflows and temperatures (v) engine operational features and constraints
<i>Step II</i>	<i>Establish design aim appropriate for current application</i> e.g., noise emissions, pollutant emissions, fuel economy, power optimization etc. Note: such requirements normally conflict.
<i>Step III</i>	<i>Develop an initial system design</i> (i) Based on simple models of component acoustic behaviour, (ii) or on data sheets and nomograms which codify and summarize experience, (iii) or on bench test data for sets of "standard" components, adjusted for flow and temperature.
<i>Step IV</i>	(a) <i>Assess acoustic performance</i> of initial design, then (b) <i>Optimize</i> by introducing systematic changes in detail (i) Use interactive computer programme, or (ii) Data sheets guided by past experience.
<i>Step V</i>	<i>Prototype validation or development</i> (i) Build and validate first prototype. Note: with one off and large industrial applications the procedure ends with this design. Otherwise, when necessary (ii) Refine the design guided by new data from (i) with appropriate theoretical predictions. (iii) Build and validate second prototype and so on. Note: one or two such iterations is normally sufficient.

first two concerned with data assembly and specification of an appropriate design aim. The third step is concerned with the development of an initial design, and the fourth with performance assessment, and then system refinement guided by more realistic computer-based calculations or their equivalent. The last step concerns the development and testing of a prototype system along the lines of the procedure summarized in Appendix A, while the whole process applied to the design of an exhaust system was illustrated in Figure 1.

One notes that the basic requirements of such a design procedure include facilities for noise measurements, a basic understanding of the acoustic behaviour of the system as a whole, with that of its constituent elements, and appropriate computer software for realistic acoustic modelling and performance prediction. Despite the obvious advantages of an integrated approach to intake/exhaust system design, current procedures treat the two systems independently, so the majority of the discussion presented here will be concerned with this approach. This is based on noise emission measurements with an existing engine including its intake and exhaust manifolds, to which an existing or modified intake and exhaust system has been attached. So the design development is concerned only with those parts of the system attached to the intake and exhaust manifold flanges.

1.2. DATA COLLECTION

Appropriate procedures for piston engine noise emission measurements are summarized in Appendix B. One notes that such measurements require appropriate consideration of any contamination by acoustic sources that are harmonically related to

engine firing frequency but not to intake or exhaust noise, as well as any contamination by other background noise. One notes too that realistic measurement of intake noise signatures can present special problems in avoiding contamination by other sources. Similarly, reliable and repetitive measurements of exhaust noise signature may be subject to uncertainties associated with the small but significant fluctuations in engine speed and combustion conditions that are found to occur during practical testing, even on a test bed. The corrected noise measurements are then appropriately processed to establish the increase in acoustic performance required for the new design.

Other relevant data include the corresponding cyclically averaged mass flow of air and exhaust gas, with the associated temperatures throughout the system. Gas temperature is of particular importance both in acoustic design and performance assessment since the local value of the speed of sound has a direct influence on the acoustic behaviour of each element. The speed of sound c is proportional to $\sqrt{T_K}$, where T_K is the gas temperature, in degrees Kelvin, and also depends on the local physical properties of the gas which also vary with temperature. The acoustic behaviour of an element at a frequency f is also strongly related to the corresponding acoustic wavelength $\lambda = c/f$ (a list of symbols and abbreviations is given in Appendix D).

To complete the data set for a specific application, one requires the relevant geometrical constraints defining volumes, lengths and cross-section areas that are available for silencing units, with the routes for connecting pipes including bends etc. This then covers the collection of the data and the establishment of the design aim in terms of the increase in system acoustic performance required, that is the first two steps in Table 1. The next two steps concern the development of an appropriate acoustic design followed by its optimization and validation in step five.

2. ACOUSTIC DESIGN DEVELOPMENT

A rational acoustic design depends on a clear understanding of the acoustic behaviour of the individual system elements as well as that of the system as a whole. The acoustic characteristics of both the system and its individual elements are determined primarily by their geometry. Essentially this consists of a series of uniform pipes connecting geometrically complex elements, including silencers, that are spaced along the flow path from the primary source of excitation at the valves to an open termination where the sound is radiated. As indicated in Figure 1, the control of intake or exhaust noise emissions for automotive application involves making the choice of appropriate silencer units, or acoustic filters, configured to fit within the spaces allocated for them during initial vehicle layout. Some common generic types, which may be packaged together to form a complete silencer box or unit, are illustrated in Figure 2. One can see that some geometric features such as expansion chambers and perforated pipes are normally common to them all, while others such as baffles, fibrous sound absorbing packing, etc. will only feature in some of them. The “tailpipes” connecting each chamber or silencing element to its successor have been omitted, but one should note that these will have a significant influence on their “installed” acoustic behaviour (see, for example, Appendix C2) and thus on the overall system performance. It turns out that virtually any complex geometry, with its acoustic behaviour, can be modelled as a train of simple elements operating in sequence or in parallel. Thus the trifold unit in Figure 2, for example, can be broken down into a sequence of simple elements. These include a perforated pipe leading to a flow reversing expansion chamber with an attached resonator which is followed by two more perforated pipes acting acoustically both in series and in parallel with the first, which then connect with a second flow reversing expansion.

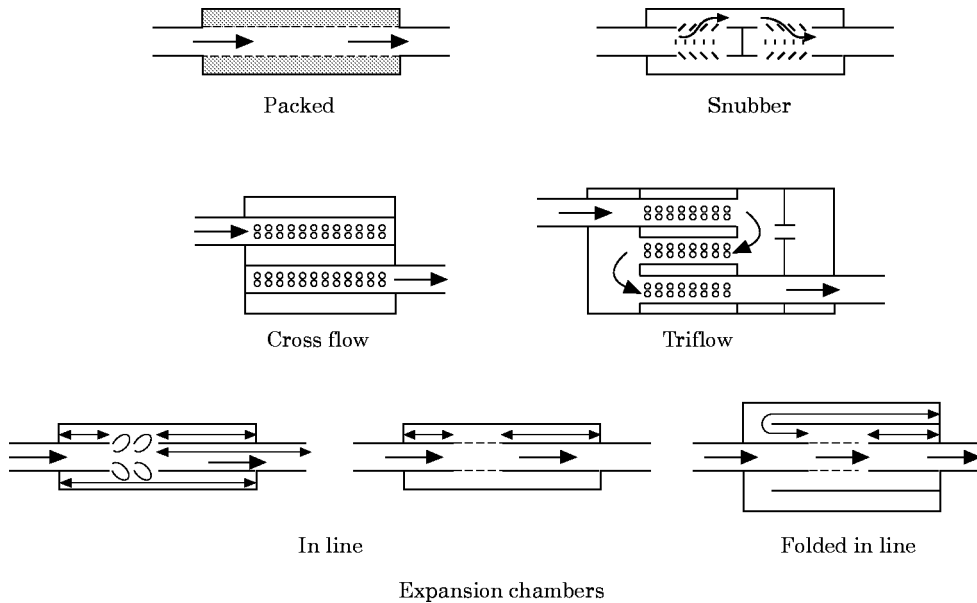


Figure 2. Silencer chamber types.

Wave reflection occurs at the junctions between each element, so the associated fluid motion consists of interfering waves superimposed on a mean flow. Thus the acoustic behaviour of all pipes is reactive, while that of the intake and exhaust systems and of their individual elements is also reactive to a variable extent. Considerable simplification of the acoustic modelling of their behaviour [3, 4] is obtained by assuming that the positively and negatively travelling component wave motions are plane and propagate without change of shape, that is as acoustic disturbances.

The filter characteristics of each silencer unit are often established by measurement and recorded on data sheets, or may be calculated by using appropriate analytic modelling [3–11]. Since the elements interact acoustically with each other, realistic acoustic performance prediction for the system is often more appropriately calculated with the analytic models, rather than the measured behaviour of the individual elements. An outline of such modelling techniques and the associated performance prediction is set out in Appendix C. Analytic models for the elements illustrated in Figure 2 can be found there, or in references [3–8].

2.1. ACOUSTIC CHARACTERISTICS OF SILENCER ELEMENTS

The acoustic behaviour of most intake and exhaust system elements is essentially reactive, but separated flow or flow reversal, perforations, fibrous packing and baffles may all enhance the resistive contribution to their performance in roughly the order listed. Reactive spectral behaviour is cyclic, exhibiting attenuation minima each time an acoustically significant length corresponds to an integer multiple of half the acoustic wavelength of the excitation, as illustrated in Figures 3 and 4. The appropriate lengths for most of the examples in Figure 2 include that of the expansion, the tail-pipe and the lengths of any side-branches. Since several lengths are thus involved simultaneously, a simple parametric description of their overall acoustic performance is not normally possible, particularly when the influence of the tail-pipe and its termination impedance is included.

However, their general ranking in terms of relative attenuation per unit volume and relative pressure loss or back pressure has been established from experience.

In automotive applications the overall acoustic performance is controlled by the attenuation minima, whenever these correspond to one of the frequencies of excitation. With stationary piston engines this correspondence can often be avoided by appropriate design. Acoustic resonance is damped by adding resistance, so the performance at attenuation minima can be improved by enhancing this factor in the design. Since space is often restricted the lowest frequency components are normally the most difficult to control.

The relative efficiency of packed silencers is roughly proportional to the packing density, the flow resistance of the pack and the other acoustic properties of the fibrous material. Their attenuation performance tends to rise significantly with increasing frequency, in correspondence with the acoustic properties of the pack, while they normally exhibit low back pressure. Their relative volumetric efficiency can be high, but tends to deteriorate in service due to fouling and disintegration of the pack. They are also relatively heavy and may cause suspension problems or may excite mechanical vibration of the vehicle structure.

The relative acoustic efficiency of snubber, baffle or cross-flow silencers is closely related to the back pressure or flow losses they generate, which often tend to be high. Their behaviour remains significantly reactive so that high acoustic efficiency is often restricted to specific sections of the frequency spectrum. Cross-flow silencers are obviously more compact than the other type, and so can have relatively better low frequency attenuation performance for the same overall dimensions. The acoustic influence of perforated pipes diminishes as the porosity increases while observation suggests it becomes negligible with grazing flow at Mach numbers less than 0.2 when the porosity rises above 15%. On the other hand, low porosity implies high through-flow losses, so a formulation of the most effective practical configuration may be difficult. Finally, these silencer types can be significant sources of flow noise, particularly at higher frequencies.

Triflow mufflers are popular, relatively compact and have a high relative acoustic efficiency. Their behaviour also tends to be strongly reactive at low frequencies so regions of poor attenuation performance are often improved by adding resonators to the flow reversal chambers, as indicated in the example in Figure 2. Back pressure losses are directly related to the changes in flow momentum at flow reversal and vary as the square of the engine speed; thus they can lead to undesirable reductions in peak engine performance. Vortex shedding at the flow reversals may also introduce significant flow noise. The observations concerning the acoustic behaviour of perforated pipes also apply to these units.

The acoustic behaviour of expansion chambers which include side branch resonators forming the bottom group in Figure 2, is discussed in the next section. They generally exhibit the lowest back pressure. The acoustic performance at low frequencies can be enhanced by adding a folded side branch, which acts in a similar manner to the resonator included in the triflow muffler example.

2.2. SIMPLIFIED MODELS OF SIDE-BRANCH RESONATOR PERFORMANCE

Simplified representations of the approximate acoustic performance of silencer units are clearly of direct assistance when laying out an initial system design. Such descriptions can take the form of simplified analytic models as set out in Appendix C2, of spectral descriptions of either measured or calculated attenuation performance, or a sequence of nomograms, performance charts, etc. Note that when such measured data is used for

exhaust system design it should be appropriately rescaled to compensate for any change of sound speed and wavelength with temperature. In all cases the information is most useful when it relates the attenuation spectrum and similar acoustic characteristics to the relevant geometric and structural features of the silencing element. This normally applies only to simple systems.

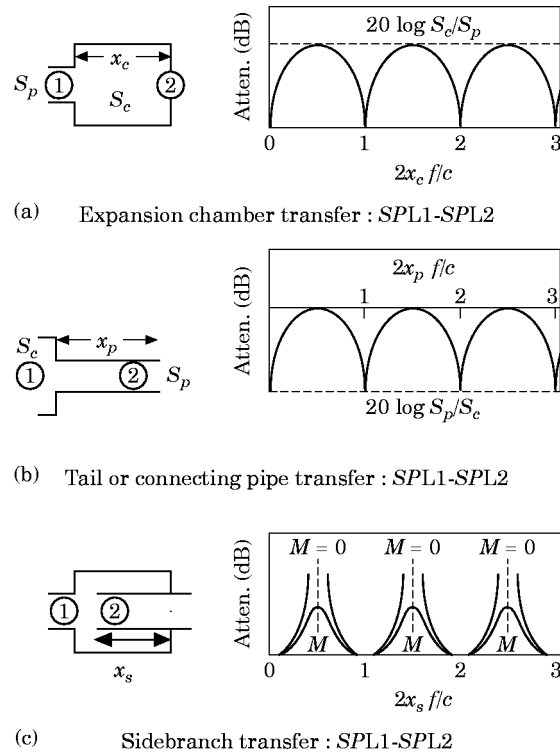


Figure 3. Approximate acoustic performance. (a) Expansion chamber transfer: $SPL1-SPL2$; (b) tail or connecting pipe transfer: $SPL1-SPL2$; (c) sidebranch transfer: $SPL1-SPL2$.

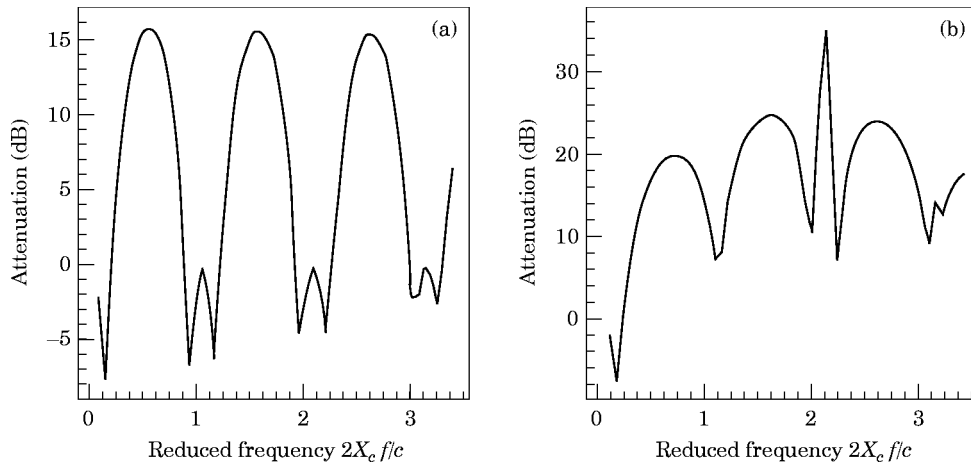


Figure 4. Attenuation of expansion chambers. (a) $X_p = X_c$; $20 \log(S_c/S_p) = 15.9$; (b) with two sidebranches: $X_s(1) = 0.5 X_p$; $X_s(2) = 0.5 X_s(1)$; $X_p/X_c = 1$; $20 \log(S_c/S_p) = 15.9$.

Such spectral distributions of the acoustic behaviour of expansion chambers with side branches are directly related to the lengths of the chamber and side branches and also to that of the tail-pipe connecting it to the next silencing element along the system. They are also influenced by the junction or termination impedance. The relative amplitude of the attenuation maxima for chambers, or minima for tail-pipes, is closely related to the chamber/pipe area ratio. The overall acoustic behaviour is the result of a summation of the interacting contributions from all constituent components of the silencer or muffler unit. However, assuming initially that they can act independently of each other provides useful insight into their relative influence on acoustic performance. This is illustrated in Figure 3 where attenuation expressed as $SPL_1 - SPL_2$ is plotted against reduced frequency $2xf/c$ or $2x/\lambda$ for each of them. One notes that the attenuation spectra for the chamber and the tail or connecting pipe follow an identical pattern of repeated maxima and minima, though that for the chamber is always positive while that for the other always remains negative. One notes too that the minima occur at integer values of the reduced frequency, while the ratio of the maxima to minima is $20 \log_{10} S_c/S_p$.

Their combined performance, after adopting an open termination and making their lengths equal for simplicity of illustration, is plotted in Figure 4(a). This demonstrates clearly how the negative contribution from the tail-pipe degrades their combined attenuation performance, particularly at those frequencies where a minimum in their individual contributions occurs simultaneously. Thus, where possible, one should avoid such coincidences by satisfying the following inequality.

$$X_c/i \neq X_p/j, \quad i, j = 1, 2, 3, \quad (2.1)$$

for the allocation of expansion chamber or tail-pipe lengths X_c , X_p during the initial design layout. The effective or useful attenuation bandwidth, defined say as the proportion of the frequency interval between minima that the attenuation spectrum exceeds half its maximum value, is also of practical interest. For the example in Figure 4(a) one sees that this is about one-half. Such attenuation performance for a single chamber may still prove acceptable when the engine speed is fixed, so that the attenuation maxima at frequencies fixed by the system geometry can be tuned to correspond with the primary engine breathing noise spectrum. But with the variable engine operating speed required for road vehicles and other prime movers, it is clearly unacceptable.

Returning to Figure 3, one sees that the attenuation spectra of side branches also exhibit a pattern of maxima and minima, with the minima again at integer multiples of the reduced frequency. Here the attenuation is always positive, but with high maximum values that are ideally infinite being restricted only by acoustic damping, which is found to increase with the Mach number u_0/c of the mean flow with velocity u_0 . Since spectral measurements are often described in one-third octave bands, a similar value can be adopted for the useful attenuation bandwidth of a side branch. One notes too that the maximum attenuation of all three components of expansion chambers occurs when

$$X/\lambda = n/4, \quad n = 1, 3, 5, \dots, \quad (2.2)$$

which provides a design criterion for the choice of optimum component lengths for well tuned expansion chamber silencers.

The combined performance of an expansion chamber with the same ratio of chamber to tail-pipe length, but now with two appropriately scaled side branches added, is illustrated in Figure 4(b). When this is compared with Figure 4(a) the marked improvement in attenuation performance for the same overall chamber and tail-pipe dimensions is obvious. The lengths of the side branches were chosen so that the attenuation peaks of the longer one correspond to the minima of the chamber and tail-pipe combination

and the first peak of the shorter one lies between those of the longer side branch. Note too that the effective attenuation spectrum is almost continuous, thus providing the wide bandwidth that is required when engine operating speeds vary significantly in service.

The comparison of Figures 4(a) and 4(b) not only demonstrates the improvement in performance within the same space resulting from the addition of side branches, but also that the side branches provide the more significant contributions to the overall performance. Therefore, to simplify the calculations for the initial design, these can be restricted to the contributions to the acoustic performance by the side branches, with any further contributions from the chamber and tail-pipe being ignored and all acoustic interactions neglected.

A similar set of simplified design criteria is not normally available with the other types of silencer illustrated in Figure 2, since as well as component lengths, several further parameters have a significant if not major influence on their acoustic behaviour and performance. Furthermore, the acoustic interactions that exist between such muffler units and their connecting pipes also introduces uncertainties, even when their individual performance can be appropriately represented or modelled [8, 9]. Although the pipes connecting silencer units always influence the system behaviour, experience indicates that the final tail-pipe length always has a significant influence on overall system performance which may be seriously degraded when its length is not well chosen.

2.2.1. Resonators and folded side branches

Resonators are used to provide attenuation at low frequencies, or to eliminate undesirable deficiencies in system performance at particular frequencies. The classical description of Helmholtz resonator acoustic behaviour is often based on an analogy that can be drawn with tuned vibration absorbers for mechanical systems. The pressure fluctuation in the resonator volume then represents the elastic restoring force with the inertia of the oscillating flow through the restriction or neck providing the equivalent mass. However, this simple lumped mass and stiffness model ceases to be realistic when the acoustic length of the resonator exceeds one-quarter of the acoustic wavelength, though the fundamental resonance may still tend to dominate the performance. A more realistic description of resonator behaviour appropriate for intake/exhaust system design is to calculate its equivalent acoustic length [3] and then treat it as a tuned side branch.

Folded side branches, as illustrated in Figures 5(a) and 5(b) provide a compact method of packaging the acoustically long side branches required at low frequencies into relatively short expansion chambers. This requires the chamber cross-section to be 10 to 15 times that of the pipe, so is only possible when space constraints allow this. In Figure 5(a), the chamber is sub-divided into inner and outer annuli, with lengths X_i and X_o and corresponding areas S_i and S_o , respectively, surrounding the pipe with internal diameter d . The cross-section shapes of the annuli have little influence on the acoustic performance, so that elliptical and other sections can be adopted to optimize the use of space. But such alternatives may enhance sound radiation from the outer surface. To accommodate the end corrections associated with acoustic wave transfer across discontinuities (see Appendix C5) the length of the radial connection between inner and outer annuli should be around $0.5d$ while that of the gap between the inlet and outlet pipes should exceed $1.5d$, which specifies the minimum value of the factor b in Figure 5. The effective acoustic length l_s of the folded side-branch is expressed to a fair approximation by

$$l_s = X_i + (S_o/S_i)X_o, \quad (2.3)$$

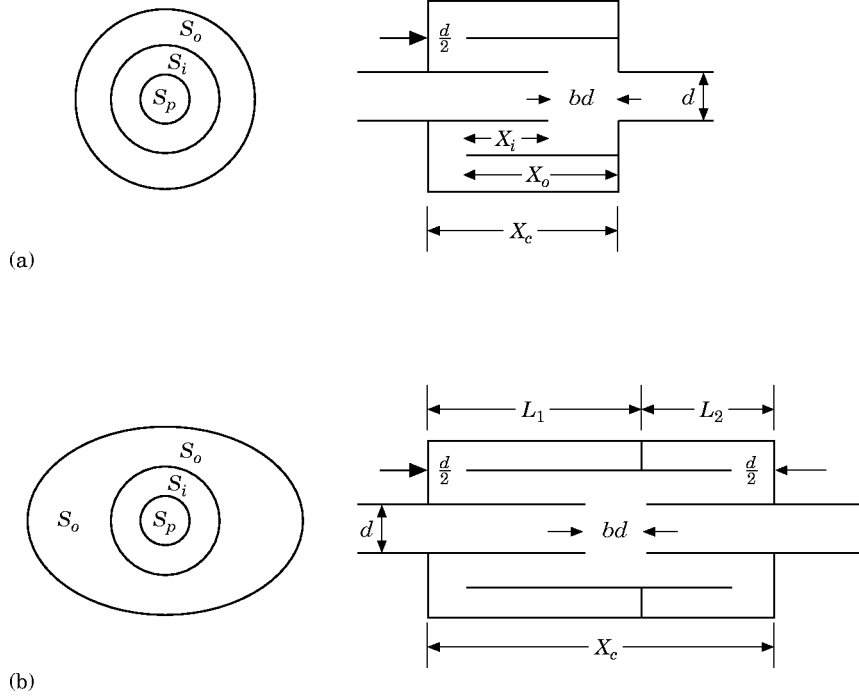


Figure 5. Expansion chambers with folded side branches. In (b) the entrance to the exit pipe is at the plane between L_1 and L_2 .

so long as S_o/S_i is less than two. Otherwise it has been found that the effective length l_s becomes progressively less than this as the area ratio increases. During performance optimization the resonator filter can be tuned by varying the diameter of the shell separating the two annuli, and thus the ratio S_o/S_i , leaving all other dimensions unaltered. Since the performance, as for a simple expansion chamber, is proportional to the ratio S_i/S_p , this may be accompanied by a small loss of peak performance as the ratio S_o/S_i increases and hence S_i/S_p decreases.

Space permitting, two folded side branches may be packaged into one silencer box as shown in Figure 5(b) to increase the attenuation bandwidth as in Figure 4(a). The available length X_c may be apportioned appropriately into two sub-units of length L_1 and L_2 . One can readily establish from the geometry shown in the figure the inequality

$$L_1 + L_2 < X_c, \quad (2.4)$$

with

$$l_1 = L_1 - bd + (S_o/S_i)(L_1 - d/2), \quad l_2 = L_2 - (d/2) + (S_o/S_i)(L_2 - d/2), \quad (2.5a, b)$$

which can be solved for L_1 , L_2 and S_o/S_i for given values of the effective acoustic lengths l_1 , l_2 and the pipe internal diameter d . A proper allowance for the wall thickness should be included in the area ratio calculations. Appropriate tuning during optimization may be performed by adjusting all, or any one, of the ratio S_o/S_i , the axial positions of the gap in the pipe, or the axial position of the baffle separating L_1 and L_2 , while leaving the overall dimensions constant.

2.3. LAYOUT OF AN INITIAL DESIGN

The majority of piston engines are employed in vehicle propulsion, where the intake and exhaust noise emission is strongly dependent on engine rotational frequency and power output. Thus the intake or exhaust system attenuation spectrum must be continuous over a wide band of frequencies. Secondly, the elements of the system must fit within the space constraints set by the overall vehicle design, which normally has been established beforehand. For example, one empirical though not necessarily realistic rule for specifying the total silencer volume required is to relate this to the swept cylinder volume. The two factors concerning attenuation and space imply that effective design for vehicle application generally represents a challenging acoustic design problem. Such problems can be severe for intakes since the allocated space is often highly restricted. The fact that the gas temperature and associated sound speed falls along the exhaust system from manifold to outlet, and also that the temperature distribution will change with engine load and speed and with road speed, gear ratio and ambient conditions, will introduce special problems for exhaust design.

The systematic design procedure set out in Table 1 and Figure 1 is based on a comprehensive range of silencer options, such as those in Figure 2, together with the codified data on their acoustic performance and other relevant characteristics. The initial design is the result of a feasibility study, which begins a design layout by listing the number, position and external dimensions of all silencer boxes with their connecting pipes that will fit within the available space. It continues with a rational choice of those silencer types or options that experience indicates are likely to produce the specified attenuation without incurring excessive back pressure or other penalties. It is also desirable that there should be simple parametric models of the acoustic performance of their components. We have seen that a fair approximation to the acoustic performance of side branch expansion chambers can be calculated simply in terms of the lengths of the side branches. It was demonstrated in Figure 4(b) that, when the lengths are appropriately chosen, an expansion chamber with two side branches has a continuous attenuation spectrum of at least 10 dB at moderate (6:1) area expansion ratios, while the back pressure produced is relatively low. Since they meet all the requirements just listed we shall adopt this type for any illustrative examples that follow. One notes that if the acoustic performance remains deficient after system optimization, then such simple units can be replaced with an alternative type that exhibits a higher volumetric acoustic efficiency, in spite of any associated back pressure penalties it may entail.

2.3.1. *Choosing leading parameters for silencer elements*

In assigning appropriate lengths l_i to the individual side branches, one notes from equation (2.2) that each side branch has attenuation maxima at frequencies corresponding to $4l_i = n\lambda$, $n = 1, 3, 5, \dots$, while $\lambda = c/f$. Thus the tuning is directly related to the sound speed c as well as to the side branch length. With intakes this is constant, but with exhaust systems it falls progressively from manifold to outlet so, for simplicity, during the initial layout calculations we shall adopt a constant reference value c_r which is an appropriate mean value. This is justified initially since interactions have also been neglected, while later optimization calculations with a computer program will adopt the appropriate local sound speed for the performance predictions and also take account of acoustic interactions between the elements.

Clearly, the longest side branch of length l_1 will provide the attenuation required at the low frequency end of the spectrum. Practical experience indicates that space restrictions often mean that this is the most difficult part of the noise spectrum to silence effectively.

Thus assignment of side branch lengths should begin say at the lowest one-third octave band with centre frequency f_r . The corresponding side branch should be tuned to this frequency so that

$$l_1 = c_r/4f_r. \quad (2.6)$$

One also notes that this side branch will produce an attenuation spectra with useful attenuation at frequencies $3f_r$, $5f_r$, etc. One then assigns the remaining side branch lengths so that their combined performance provides a continuous spectrum of high attenuation. They combine most effectively when their lengths form a geometric series, so that successive lengths are in the ratio

$$l_{(i+1)}/l_i = 3^{(-1/m)}, \quad i = 1, 2, 3, \dots, (m-1), \quad (2.7)$$

where m is the total number of side branches. When space permits, two or more side branches can be accommodated in series in a single box, while the longest ones will probably be folded. Optimum packaging considerations normally fix the sequence in which they are installed along the system, but this can modify the acoustic performance, since the lengths of connecting pipes between boxes is extended by the side branches. The best sequence can be decided during optimization.

2.4. PREDICTIVE TECHNIQUES APPLIED TO SYSTEM DEVELOPMENT

Adoption of rational predictive techniques can enhance the quality of intake/exhaust design and greatly reduce development time. Valid predictions must always include the influence of acoustic interaction between component elements, of mean flow and of gas temperature (see Appendix C). They should, where possible, include the influence of interaction between the system and primary sources at the valves with noise generation elsewhere by turbulent flow and vorticity (flow noise) and any flanking transmission. Thus, for vehicle applications, prototypes are normally built and tested to validate the design. This is hardly feasible for large industrial or “one off” designs, since the associated cost is then prohibitive.

System performance refinement begins with an acoustic assessment of the initial design layout. A program that first calculates the relative amplitudes of the incident and reflected waves at say each area discontinuity is perhaps the most useful (Table 2). Such information then directly provides the impedance, reflection coefficient and other relevant spectral acoustic data at many locations along the system. This also allows the designer to assess the relative contributions of each individual element to the overall system performance. At this stage, for example, the attenuation performance spectra of the system and of its components can be defined according to equation (C10) in Appendix C. Such theoretical predictions can be used to ascertain the likely effect of systematic modifications to the system detail design and layout, thus minimizing the number of expensive prototype stages required. Each step of this development provides additional insight into system behaviour to guide the development of further appropriate changes to refine the design.

Flow noise has been found to have a major influence on the maximum attenuation achieved under operating conditions. Since its influence is not normally included in theoretical performance assessments, any such predictions suggesting a very high attenuation performance may be unrealistic [9, 12] and thus misleading. Experience indicates that design modifications concentrated on increasing attenuation where acoustic theory predicts a minimum usually lead most rapidly to improvements in installed performance. Theoretical predictions can also be used to enhance the detailed design stages, allowing rapid design refinement of the first prototype.

TABLE 2

Theoretical calculation of system performance

<i>Step I</i>	<i>Assemble relevant data</i>
	(i) System layout, geometry and relevant structural features.
	(ii) Cycle averaged mass flow for intake and exhaust.
	(iii) Ambient and other relevant operational conditions.
	(iv) Cycle averaged exhaust valve outlet temperature and gas species.
	Note: Step (iv) concerns exhaust systems only.
<i>Step II</i>	<i>Calculate exhaust flow and temperature distribution</i>
	(i) Calculate hot surface area of system elements.
	(ii) Estimate relevant heat transfer coefficients.
	(iii) Estimate flow temperature distribution.
	(iv) Estimate static pressure and Mach number distribution.
	Note: Steps (ii)–(iv) require iterative calculations.
<i>Step III</i>	<i>Evaluate acoustic wave propagation at each frequency</i>
	(i) Choose appropriate analytic model for each element.
	(ii) Starting at the open termination calculate the relative incident and reflected wave amplitudes throughout the system for the relevant systematic sequence of frequencies.
<i>Step IV</i>	<i>Describe system performance</i>
	(i) Present acoustic impedance and reflection coefficient spectra.
	(ii) Present attenuation and insertion loss spectra.
	Note: alternatively, sound emissions may be presented for each engine order versus r.p.m.
	(iii) Present system back pressure or flow losses at relevant operating conditions.

Other assessments of system performance can be useful at this stage. When the source volume velocity and impedance are known, the predicted insertion loss (see equation (C9)) provides a useful index to guide the final design assessment, as it often corresponds to direct measurement. Note, however, that this index relates to the system as a whole and gives little insight into the contributions of individual components. The influence of flow noise can also be minimized by attention to flow path detail design as can the flow losses or system back pressure.

As well as validating the design, the fabrication and testing of a prototype provides useful insight into the system behaviour. The results provide additional data to guide any further modifications that may be necessary. Theoretical predictions can usefully be adopted to assess and refine designs directly on the vehicle. This now includes the consideration of mounting attachments, noise radiated from system surfaces and associated vehicle noise transmission characteristics. Such an addition to the total noise emission by the system is often called flanking transmission.

2.5. THEORETICAL PREDICTION OF SYSTEM PERFORMANCE

Realistic predictions of the acoustic behaviour with the associated characteristics of system performance form an essential part of any rational design process. As well as spectral descriptions of acoustic behaviour, the calculations should provide estimates of the system back pressure or static pressure loss. As well as the geometric and other structural features of the system, the acoustic characteristics depend on the distribution of flow temperature and Mach number, so these must be established first.

Thus the first calculation to be made concerns the temperature distribution, which in turn is a function of the cycle averaged mass flow and temperature of the gas leaving the exhaust valve with its physical properties, the ambient conditions surrounding the system with its geometry and relevant structural features. The temperature distribution depends

on the heat transfer from gas to system boundaries and thus on the associated heat transfer coefficients. Since these also depend on the Reynolds and Prandtl numbers in the flowing gas at the boundaries, the calculations are necessarily iterative. The Mach number is also a function of temperature and flow velocity which depends on the local gas temperature, so the Mach number calculations are those appropriate to compressible flow with axially varying static temperature.

Once realistic estimates of temperature and Mach number have been established then the relevant acoustic spectral characteristics can be calculated at one frequency at a time, starting at the open termination and progressing to the valves [3, 13]. This requires appropriate analytic models of each element in the system [4] that have been incorporated into computer programs that run, say, on any small desk top machine. Suitable Fortran programs are available for this purpose.

3. SELECTED EXAMPLES OF INTAKE AND EXHAUST SYSTEM DESIGN

The application of the rational design procedure, summarized in Table 1, to the control of noise emission from intake and exhaust is demonstrated by a sequence of practical examples. Experience with the many different applications listed in the second paragraph of the introduction indicates the general applicability of the approach to successful acoustic design. Of these, the smallest was a 1 cc displacement model diesel and the largest a 30 MW electric generator! Some representative examples have been selected from this list. The first concerns the control of boom in the cabin of a current production pick-up truck, by the suppression of noise emission from the intake pipe. The second concerns the development of a low back pressure exhaust system to improve the performance and economy of a production car. The third concerns the control of high noise levels experienced on the sun deck of a passenger ship from the main engine exhausts, while the fourth concerns the development of an optimized system with high acoustic performance for the original Quiet Heavy Vehicle project. The last two are also documented in the literature.

The designs chosen all have the common feature that the noise control filters consist of side branch expansion chambers which were discussed in sections 2.2 and 2.3, and are thus directly relevant in that context.

3.1. CONTROL OF INTAKE NOISE EMISSION

The problem arose in connection with a pronounced boom with a level of 85 dB(A) and centred at 114 Hz that was experienced in the driving cab of a small pick-up truck at full throttle with engine speeds around 3400 r.p.m. This corresponded to the firing frequency or second order (2E) of the engine rotational frequency. The boom frequency corresponded to fast cruise in fifth gear at 120 km/h and equivalent road speeds in lower gears, with a corresponding impact on vehicle quality. Acoustic investigations demonstrated that a strong vertical mode existed in the cabin at 120 Hz, while a pronounced acoustic resonance occurred in the engine compartment centred around 95 Hz. They also traced the source of the body boom to the sound emitted at the open end of the intake pipe.

To control the intake emissions at or near 114 Hz, sufficient space was available in the engine compartment to replace the 48 mm diameter intake pipe with a re-sited and appropriately tuned expansion chamber resonator 240 mm long with a maximum diameter of 200 mm (see section 2.2.1). The design followed the approach set out in Table 1 with the configuration shown in Figure 5(a) being used. At the local ambient conditions, the

acoustic wavelength at 114 Hz is 3.07 m, giving the necessary effective sidebranch acoustic length l_s of 0.77 m according to equations (2.2). From equation (2.3), the maximum chamber length available suggested that an area ratio S_o/S_i of at least three was required, noting that this exceeded the specified limit of two. This however provided sufficient information for dimensioning an initial design to predict its installed performance with a computer. This was found to be tuned to 160 Hz, so it was retuned to just below 120 Hz by increasing the ratio S_o/S_i to 4.55. The final design had a chamber length of 240 mm with an outer shell internal diameter of 166 mm and a bell-mouthed intake pipe 44 or 60 mm long.

The new intake dimensions and the predicted silencer performance is shown in Figure 6(a). Note that the bell-mouth entry was retained, although not shown by the drawing. The improvement in the environment within the cab resulting from the control of intake noise is illustrated in Figure 6(b), which speaks for itself!

3.2. EXHAUST SYSTEMS WITH LOW FLOW LOSSES

The influence of back pressure on vehicle performance and economy is clearly established by experience. This example forms part of a feasibility study of the likely improvements that could be obtained to these without a corresponding loss of acoustic performance. The study was confined to the lower engine size range of current production cars, where an existing system was replaced by a new design with significantly reduced pressure loss. One obvious method of doing so is to increase the pipe diameter slightly, with a corresponding significant reduction of the flow dynamic pressure. However, this implies reduced expansion ratios for the silencer boxes with a corresponding reduction of acoustic performance.

The specification restricted any new exhaust system layout to following the existing route but permitted enlargement of the boxes to occupy fully available space, but it prohibited the use of sound absorbing packing. As well as drawings of the existing system outline, together with any further volume expansion at the boxes, unsilenced (straight pipe) noise spectra were supplied for a sequence of engine speeds at full load. Mass flow and temperature distributions measured with the existing system were also provided. The noise spectra were combined to give a composite noise spectrum in one-third octave bands rescaled to 7.5 m as shown in Figure 7(a). When all 20, say, bands are silenced to the same level, then this should be less than $75 - 10 \log_{10} 20$, or 62 dB(A), to produce an overall exhaust noise level of 75 dB(A). Upon concentrating on the first 10 loudest ones, the requirement becomes 65 dB(A) (see Figure 7(a)). The difference in spectral levels represents the system attenuation required or the design aim.

The original system had two silencer boxes. The space available showed that one box could be extended in length and subdivided to give two expansion chambers, while the cross-section of both the original boxes could also be increased slightly. This gave an increase in silencer volume of some 60%, which was necessary, since the volumetric acoustic efficiency of straight through expansion chambers with side branches is somewhat lower than the relatively high flow loss types used in the original system. Thus with three chambers it was possible to install a maximum of six side branches, though five were adopted in this case, to accommodate the longest required. The length adopted in initial design layout for this was 0.7 m calculated from equation (2.6) with $f_r = 200$ Hz and $c_r = 550$ ms⁻¹. The lengths of the other five was scaled according to equation (2.7), with $m = 5$.

The initial design was transferred to the computer and then optimized for acoustic performance. Before doing so, some attention was paid to reducing back pressure by increasing the downpipe internal diameter from 32 to 38 mm with the remainder from 35

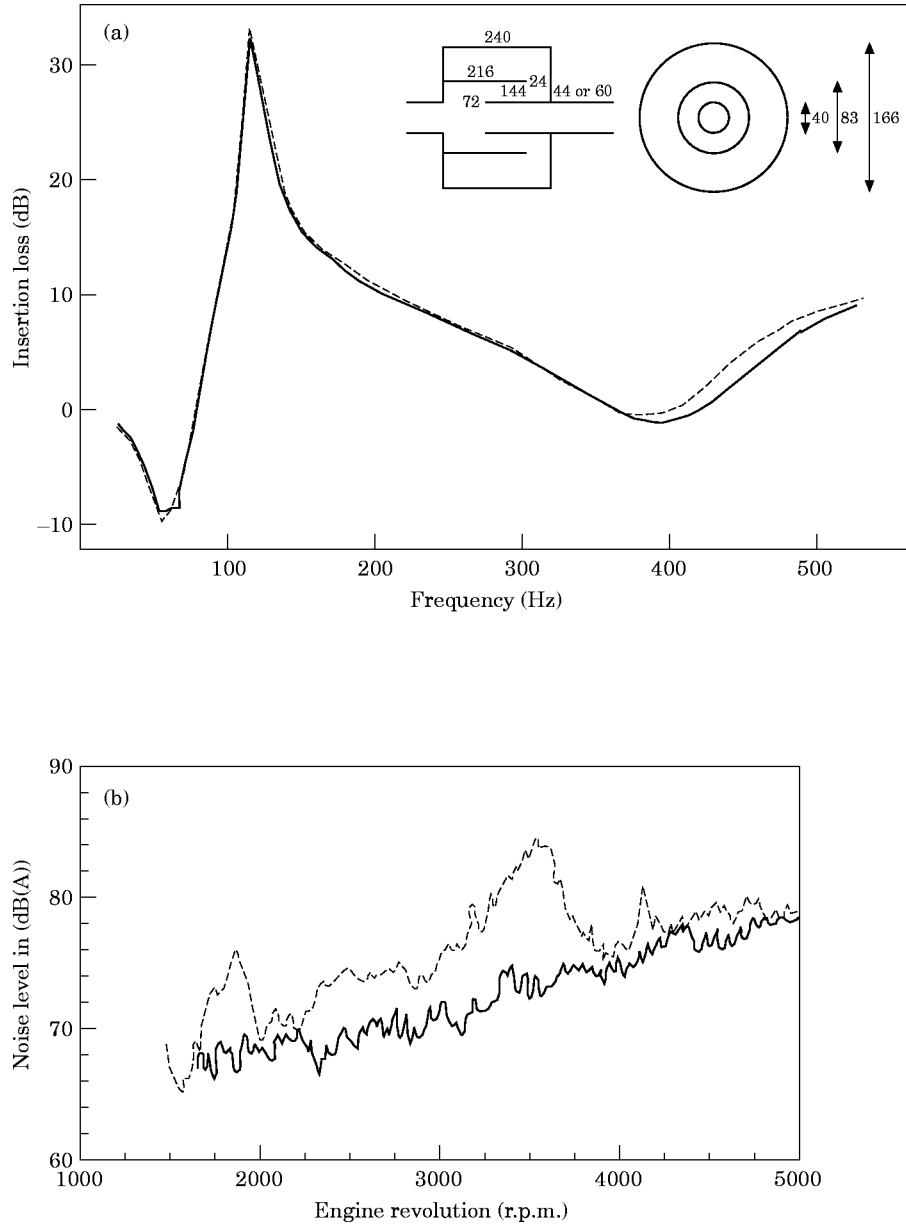


Figure 6. Overall interior noise recorded at full throttle in fourth gear. (a) Predictions for modified silencer design: —, 40 mm intake pipe; ---, 60 mm pipe; (b) noise measurements: ---, normal vehicle; —, with optimized silencer.

to 38 mm. The first prototype had an unacceptable performance at 800 Hz, though it was otherwise satisfactory. The second prototype was deemed to be satisfactory, as was confirmed by the drive by test results in Figure 7(b). The system back pressure was halved, resulting in some 20% increase in peak power and 30% improvement in fuel consumption. The maximum interior noise levels were also reduced by 5 dB at the rear seat, though the reason for this was not established. These improvements were accompanied by a modest, but acceptable increase in drive by noise levels. Although the silencer boxes were

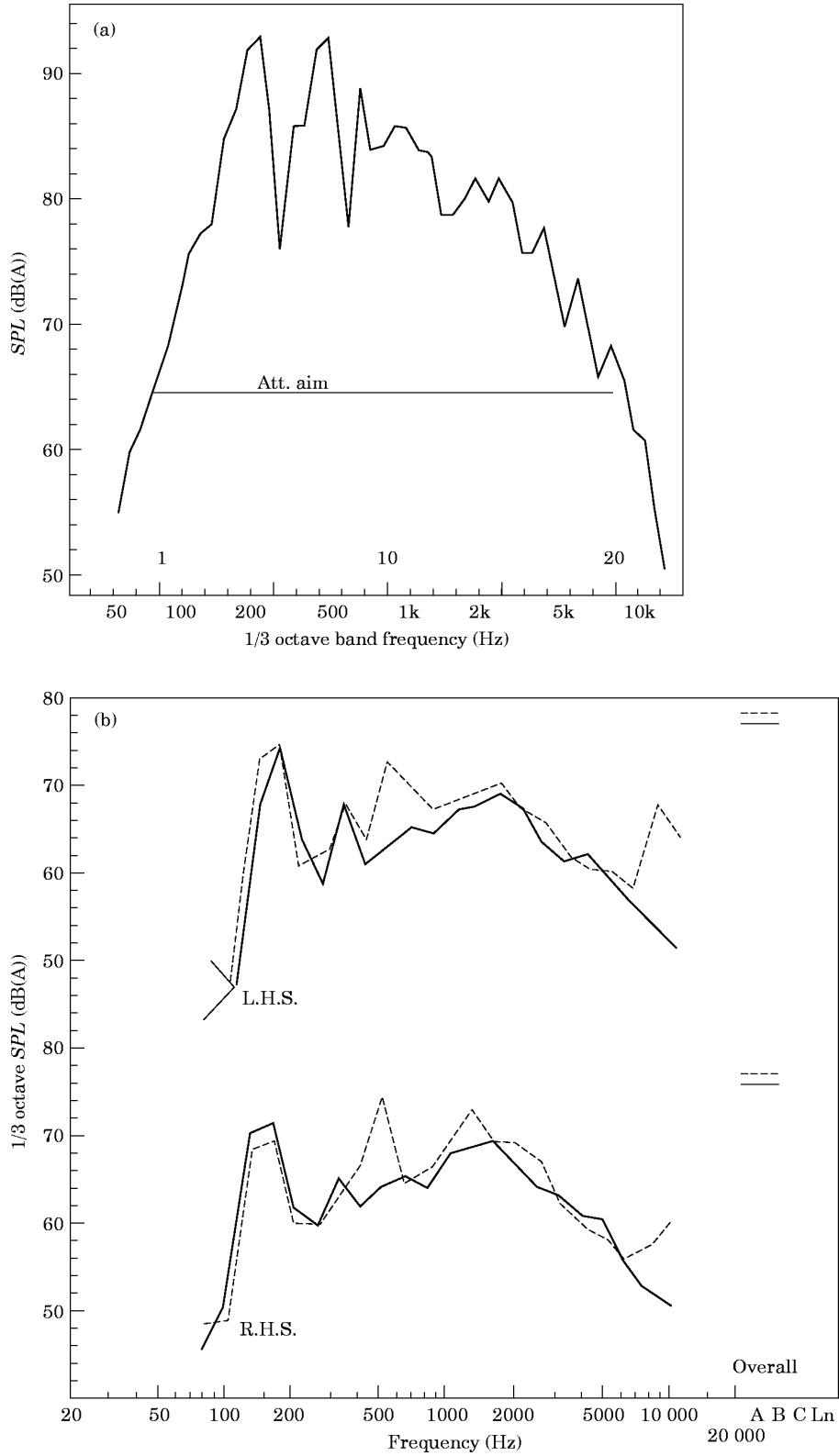


Figure 7. Exhaust noise at 7.5 m. (a) Composite spectra for open pipe, adjusted to 7.5 m from outlet; (b) Drive by measurements: —, standard; ---, ISVR design.

significantly bulkier, the relative fabrication costs and weight increase of the new system remained modest, due to the simple design.

3.3. SHIP MAIN ENGINE EXHAUST NOISE CONTROL

As built, the passenger ship concerned was not fitted with exhaust silencers on the two main turbocharged engines, which made low frequency contributions to the excessively noisy environment on the sun deck under cruising conditions. The generator exhausts, which were silenced, produced noise levels from 25 to 30 dB below that of the main engines, while the main contributions above 250 Hz came from the engine room supply fans. Observations of the engine noise emissions with the fans switched off gave levels of around 110 dB below 50 Hz, falling off sharply above this frequency to approximately 90 and then more slowly to 75 dB at 250 Hz. A weighted overall main engine exhaust noise level on the sun deck was assessed at about 85 dB(A). The fans required acoustic treatment but obviously the main engine exhausts also needed to be silenced.

The exhaust pipe was 1.1 m diameter and appropriate space for a silencer was very restricted below deck. However, by rerouting the generator exhaust stacks a sufficient but somewhat irregularly shaped space was found at the top of the funnel! This was about 4.5 m long with roughly the same cross-section as a 2.2 m diameter cylinder. During cruise the engines ran at a set constant speed driving a variable pitch propeller, so the frequency of the exhaust noise spectral components remained fixed, though their level varied somewhat. Full advantage was taken of this fact during the 22 design calculation trials with different chamber lengths and volumes, which were all tuned to attenuate the significant components. The details can be found in reference [14], so are not repeated here. The most likely option with predicted overall emissions of 65 dB(A) was built and installed, one for each engine in the corresponding funnels as shown in Figure 8. An insertion loss of 20 dB to 64 dB(A) was achieved by each of these two simple compact side branch expansion chamber silencers resulting in a combined contribution of 67 dB(A) from the main engine exhausts.

3.4. THE INFLUENCE OF FLOW NOISE ON ACOUSTIC PERFORMANCE

The last example concerns the development of a high acoustic performance exhaust system for noise control during the first Quiet Heavy Vehicle prototype development. This was aimed at determining the technical feasibility and cost of reducing the noise levels of heavy diesel-engine goods vehicles to levels some 10 dB(A) lower than the then current values. Since engine surface noise presented a major problem in achieving this goal it was decided to reduce exhaust noise emission to below the level at which its contribution was significant. Thus this was assigned an upper limit of 69 dB(A) [15], while engine turbocharger performance restricted the maximum back pressure to 45 mm of mercury.

Finding adequate space on a tractor unit for an exhaust system designed to meet this challenging specification presented an initial problem. Vehicle manoeuvrability precluded mounting it in the popular position behind the cab and the only possible free space was below the front bumper. The final design, that would first fit within the only space available is illustrated in Figure 9(a), consisted of two cylindrical boxes 0.25 m diameter and almost 2 m long. This layout required four sharp bends with their associated flow losses. To reduce the back pressure, the exhaust pipe diameter was increased from 100 to 125 mm at the entry to the 180° bend, thus reducing the flow dynamic pressure by a factor of 2.4 in the second box. The initial bend design included steady flow diffusion by distributing expansion around the bend, but in the final construction it was replaced by the abrupt expansion shown, with an associated increase in pressure loss from 25 mm to 35 mm Hg.

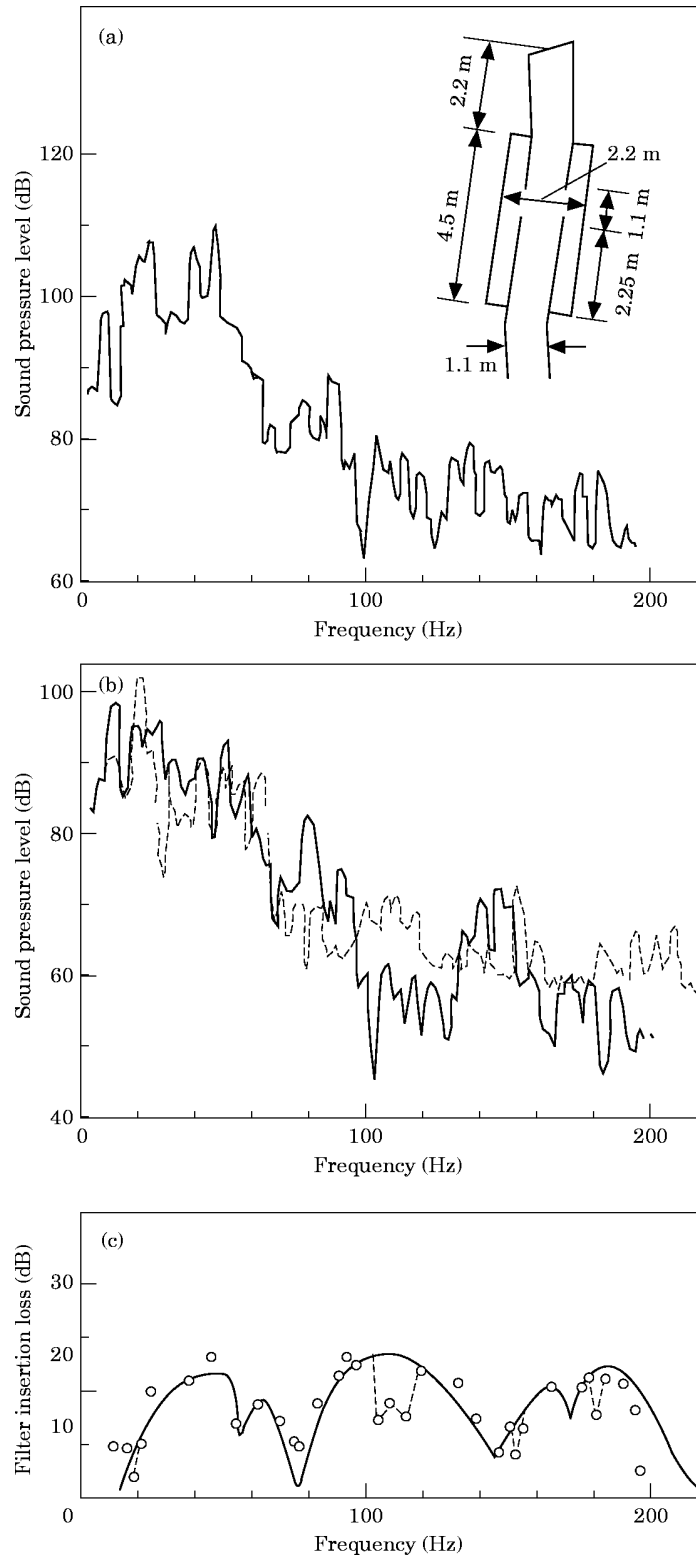


Figure 8. Insertion loss spectra. (a) Noise signature of unsilenced engine at 420 r.p.m. 3 Hz filter, NR91; 84 dB(A); (b) —, predicted silenced spectrum at 420 r.p.m. (65 dB(A)); - - -, measured spectrum at 460 r.p.m. (67 dB(A)); (c) insertion loss: —, predicted at 420 r.p.m.; \circ , estimated from silenced measurements at 460 r.p.m.

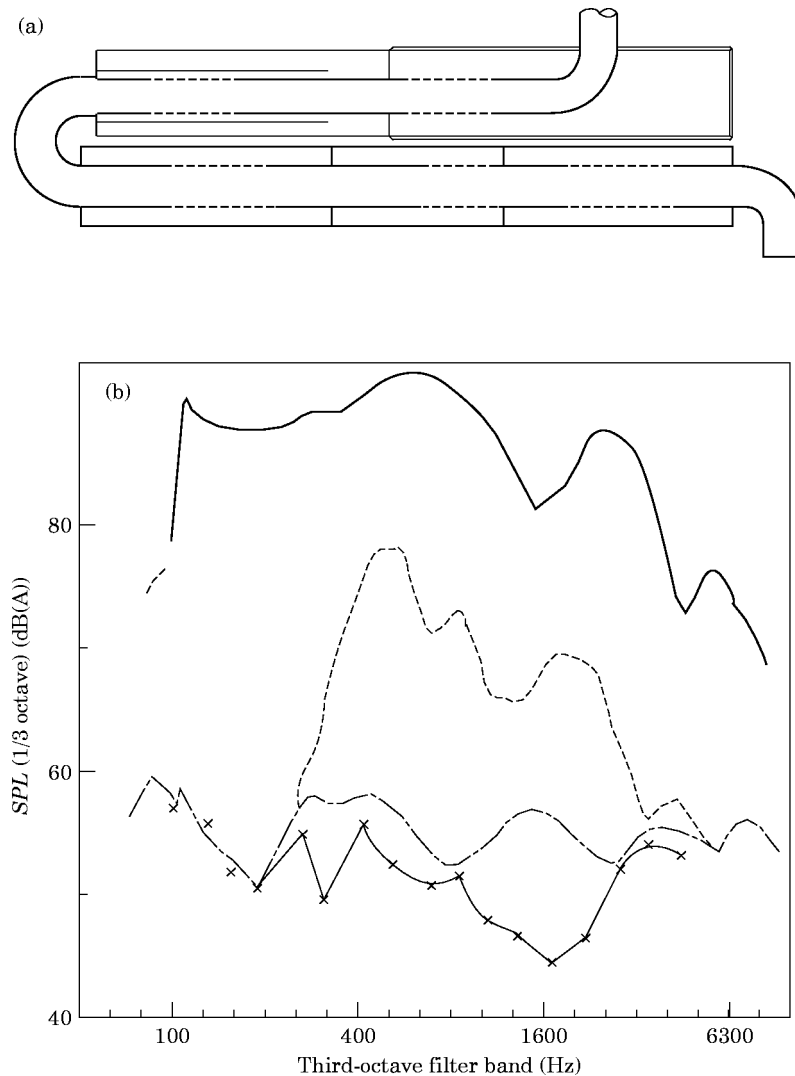


Figure 9. (a) Silencer design for Foden QHV showing perforated tube sections in extended inlet and outlet pipes (side branches). First chamber of first silencer sheathed with 3 mm asbestos and outer layer of 1.2 mm thick aluminium sheet; (b) test bed measurements at full load, adjusted to 7.5 m; averaged for eight speeds from 1000 to 2500 r.p.m; —, peak open pipe; ---, omitting perforate bridges (flow noise); —, silenced, peak measured; —x—, peak predicted.

The perforated tube sections bridging the openings between the pipe and expansion chambers also reduced the back pressure significantly as well as reducing flow noise. The influence of flow noise is illustrated in Figure 9(b) which compares three composite one-third octave band noise spectra, measured at eight engine speeds with full load, with theoretical predictions, after they have all been rescaled to 7.5 m. One should also note the good agreement between predicted and measured performance below 300 Hz, where the relative influence of flow noise is known to remain small. At any of the speeds tested the maximum emitted exhaust noise levels at full load were 67 dB(A) with the final prototype design which then increased to 69 dB(A) with the final operational version.

The choice of hole size and perforate porosity was found to have a significant influence on both the acoustic performance and the flow generated noise. The best acoustic performance was obtained with small holes and high porosity. Flow noise and pressure loss also increased with both hole and size and porosity. However, a practical limit to the minimum acceptable hole size is provided by their tendency to clog with fouling during normal service. A fair compromise that was adopted had 3 mm diameter holes with 10% porosity, though this was halved in one box for the operational version. The significant influence on silencer performance by fouling during service is described in reference [16], where it is strongly recommended that fouling should be removed by steam cleaning during regular maintenance so that the acoustic performance is maintained.

4. INTEGRATED SYSTEM ACOUSTIC DESIGN

An integrated procedure begins with a detailed calculation of the cyclic wave action throughout intake, valves, cylinder and exhaust corresponding to all conditions of engine operation. The valves and cylinder with the manifolds represent a time varying system, while the remainder of the intake and exhaust system act mainly as a passive acoustic filter. It is clear from previous discussion that this may not be strictly true in practice but represents a useful first approximation. The analysis of wave action in the time varying components of the running engine is best performed in time. However, realistic time domain descriptions of wave action in all those parts of the system with complex geometry, such as acoustic filters and the like, do not currently exist. It is clear also that realistic models of their acoustic behaviour are readily established in the frequency domain. Since the wave motion is cyclic, a time domain description is readily Fourier transformed to the frequency domain and *vice versa*. This suggests a hybrid approach to the calculation of the integrated wave action throughout the system [1, 4] as summarized in Table 3.

Since we are concerned with intake/exhaust system design for the control of noise emissions, it will again be assumed that the engine already exists with relevant test data defining power output, mechanical, volumetric and thermal efficiency, while valve design and manifold layout are already established. The concern here is to evaluate the wave action for any given speed and load.

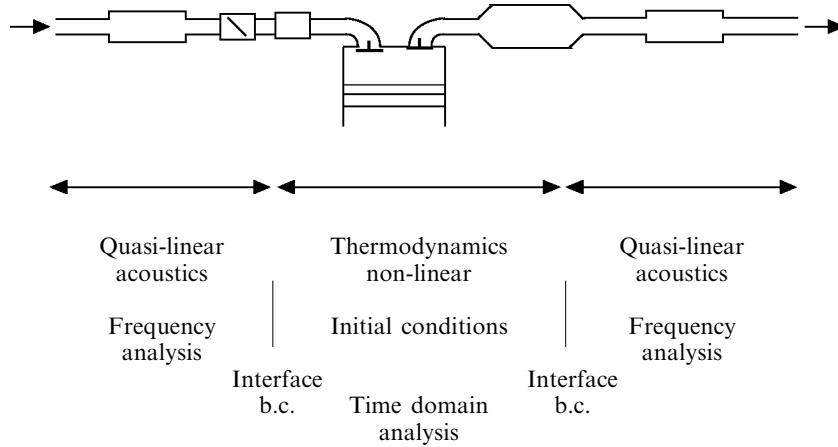
In practice any such calculations are necessarily iterative, since the time domain calculations require realistic time varying boundary conditions at the two interfaces with the filters. These are defined in time by an appropriate Fourier transformation of the corresponding acoustic reflection coefficient spectra. Such acoustic calculations require time averaged values of gas mass flow and temperature. These can be calculated initially with reference to the associated thermodynamics of the engine cycle as set out in Table 4. The time required to calculate the wave action in the manifolds is considerably reduced if an initial pressure distribution can be established there by an appropriate Fourier transform of the local acoustic impedance spectrum combined with the cyclic mass or volume velocity time history of the flow through the valves. This in turn can modify the cyclically averaged values of gas mass flow and temperature at the interfaces, since these depend on appropriate choice of the values of p_1 and T_1 in Table 4.

Practical experience [17] has already demonstrated that the hybrid approach provides realistic narrow band predictions of intake and exhaust noise emissions, along with realistic estimates of the engine breathing performance. Further details of the approach with the results of some validation experiments made with a highly tuned current production engine can be found in reference [18]. Thus, by adopting this methodology, a rational balance may be struck between optimum engine performance and reduced noise emission. The

TABLE 3

Integrated hybrid description of wave action

This can be represented as a combination of wave motion in cyclically time varying parts with wave motion in the time stationary parts. That part associated with moving boundaries and high fluctuating pressure amplitudes (non-linear processes) is best analysed in the time domain. Spectral characteristics of acoustic filters and the sound emissions are best described in the frequency domain.



Initial conditions are defined by: (i) engine cycle thermodynamics; (ii) inverse Fourier transform of acoustic impedance spectra at interface. The boundary conditions at the interface are defined by an inverse Fourier transform of acoustic reflection coefficient spectra.

TABLE 4

Initial estimates for acoustic assessments

Engine running at cyclic frequency	f_c
with compression ratio	r
power output/cylinder	P
intake temperature	T_1
intake pressure	p_1
swept volume/cylinder	V
port or pipe area	S_p
volumetric efficiency	η_v
mechanical efficiency	η_m
ideal thermal efficiency	$\eta_t = 1 - r^{-(\gamma-1)}$
polytropic index	n

For each cylinder calculate

- (1) Ideal work per cycle $W = P / \eta_t \eta_m f_c$;
- (2) Cycle constant $K = V [r / (r - 1)] \{ r^{(n-1)} - 1 \} / (n - 1)$;
- (3) Cycle index $\beta = (1 + W / (K p_1))^{1/n}$;
- (4) Cyclic exhaust volume $V_e = V [\beta (r - 2) + 1] / (r - 1)$;
- (5) Exhaust temperature $T_e = T_1 \beta$.

Values passed to acoustic programs:

- T_e to predict exhaust temperature distribution and to define exhaust gas properties;
- M_e exhaust Mach number, $V_e f_c / (S_p c)_e$;
- M_i intake Mach number, $V f_c \eta_v / (S_p c)_i$.

Note: The program will provide updated values of p_1 , T_1 , also it must check that mass flow and momentum balance is maintained.

resulting software has the distinct advantage of being sufficiently compact to run efficiently on a desk top computer.

4.1. OTHER DEVELOPMENTS

Sophisticated models of combustion and other factors describing notional engine performance already exist and form a basis for current engine design and development. The obvious next stage is to develop a completely predictive procedure for engine noise emissions and performance, by replacing measured engine performance data by predictions. Some progress in this direction seems to have already been made elsewhere [19], though relevant technical details are not available. Essentially, however, it apparently will provide similar facilities to those already available through the hybrid approach, although it does seem to require extensive computational resources.

5. LITERATURE ON EXHAUST SYSTEM DESIGN

The references cited here with the further references they include have been chosen to provide an complete and adequate description of valid intake and exhaust system acoustic modelling that is of direct relevance to design.

Much has been published by eminent authorities and others on practical or theoretical studies of system acoustic performance and exhaust noise. Unfortunately, the material to be found there is often of restricted value for direct application to rational design methodology. There are a number of reasons for this. Many theoretical and experimental studies have been concerned with transmission loss and thus have neglected the existence of interactions between components, although experience has demonstrated that these have a major influence on practical behaviour. Others omit essential experimental or structural detail when reporting the results of observations [9] so the results, though potentially useful, cannot be practically applied. For mathematical convenience others may have concentrated on simplified theoretical modelling, to the neglect of sufficient physical realism or insight, so that the solutions are not valid for practical design nor appropriate to guide decisions during the design process. For example, the influence of mean flow on system tuning and acoustic energy transport may be neglected. Similarly, the inevitable presence of evanescent waves at an area discontinuity may be omitted from the theoretical modelling. Sometimes one of these factors may be included, but not the other. Worse perhaps, some studies expound ideas or present results which are misleading. For these reasons the references selected were deliberately restricted to those found appropriate for intake and exhaust system design, although the list may then appear somewhat parochial!

ACKNOWLEDGMENTS

The author wishes to thank the referees for their helpful comments and suggestions for improving this paper.

REFERENCES

1. P. O. A. L. DAVIES and M. F. HARRISON 1957 *Proceedings of the Institute of Acoustics* **15**(3), 369–374. Hybrid systems for I. C. engine breathing noise synthesis.
2. P. O. A. L. DAVIES 1992 *ISVR Technical Report* 207. Intake and exhaust noise.
3. P. O. A. L. DAVIES 1988 *Journal of Sound and Vibration* **174**, 91–115. Practical flow duct acoustics.
4. P. O. A. L. DAVIES 1992 *ISVR Technical Report* 213. Practical flow duct acoustic modelling.

5. J. W. SULLIVAN and M. J. CROCKER *Journal of the Acoustical Society of America* **64**(1), 207–215. Analysis of concentric tube resonators having unpartitioned cavities.
6. J. W. SULLIVAN 1979 *Journal of the Acoustical Society of America* **66**, 772–788. A method for modelling perforated tube muffler components.
7. P. O. A. L. DAVIES 1993 *Noise Control Engineering* **40**, 135–141. Realistic models for predicting sound propagation in flow duct systems.
8. P. O. A. L. DAVIES 1991 *Journal of Sound and Vibration* **151**, 333–338. Transmission matrix representation of exhaust system acoustic characteristics.
9. G. D. CALLOW and K. S. PEAT 1988 *Proceedings of the Institution of Mechanical Engineers* **C19/88**, 39–46. Insertion loss of engine intake and exhaust silencers.
10. P. E. DOAK 1992 *Journal of Sound and Vibration* **124**, 945–948. Acoustic wave propagation in a homentropic, irrotational, low Mach number mean flow.
11. P. O. A. L. DAVIES and P. E. DOAK 1990 *Journal of Sound and Vibration* **138**, 345–350. Wave transfer to and from conical diffusers with mean flow.
12. P. O. A. L. DAVIES 1981 *Journal of Sound and Vibration* **77**, 191–209. Flow acoustic coupling in ducts.
13. P. O. A. L. DAVIES 1988 *Journal of Sound and Vibration* **122**, 389–392. Plane wave acoustic propagation in hot gas flows.
14. P. O. A. L. DAVIES 1973 *Proc. I.M.A.S. 73, London, Transactions of the Institute of Marine Engineers, 1974, Series B*, **4**, 59–65. Exhaust system silencing.
15. J. W. TYLER 1979 *Proceedings of the Institution of Mechanical Engineers* **193**(23), 137–147. The TRRL Quite Heavy Vehicle Project.
16. P. M. NELSON and M. C. P. UNDERWOOD 1982 *TRRL Supplementary Report* 746. Operational performance of the TRRL quiet heavy vehicle.
17. M. F. HARRISON and P. O. A. L. DAVIES 1994 *Proceedings of the Institute of Mechanical Engineers* **C487/019**, 183–190. Rapid predictions of vehicle intake/exhaust noise.
18. M. F. HARRISON 1994 *Ph.D. Thesis University of Southampton*. Time and frequency domain modelling of vehicle intake and exhaust systems.
19. M. PEAT 1993 *Noise and Vibration Worldwide* (March/April), 8–11. Expert system addresses exhaust noise and overall silencer performance.

APPENDIX A: PROTOTYPE DEVELOPMENT PROGRAMME

I. Carry out realistic assessment of initial design

- (i) Include
 - (a) mass flow, gas properties and temperatures etc.
 - (b) acoustic interaction between components
 - (c) all relevant geometric and structural features
 - (d) effective acoustic models of all elements.
- (ii) Identify all spectral regions of low relative attenuation.

II. Refine initial design to develop first prototype

- (i) Assess relative contribution of each element to overall attenuation.
- (ii) Make appropriate systematic adjustments to system layout.
- (iii) Theoretically assess their effect on raising attenuation performance.
- (iv) Make appropriate systematic changes to element detail design.
- (v) Theoretically assess their effect on raising attenuation performance.
- (vi) Restrict flow noise and back pressure by flow path improvements.
- (vii) Theoretically reassess the design at all engine speeds and loads.

III. Build and test a first prototype directly on vehicle

- (i) Compare measured insertion loss or attenuation with design aim.
- (ii) Identify areas requiring further improvement.
- (iii) Further refine design using theoretical assessments.
- (iv) Assess the influence of system mounts and surface vibration on vehicle noise (flanking transmissions).

IV. *Test and assess second prototype etc.*

Notes: (a) Uncertainties always exist due to the influence of

- (i) Flow noise
- (ii) Interactions with source
- (iii) Flanking transmission.

(b) Tests of each prototype extend the database to guide any future modifications.

APPENDIX B: ENGINE EXHAUST NOISE SIGNATURE MEASUREMENT

Purpose: To provide data with unsilenced or original system representing all operating speed and load conditions, to establish an acoustic design aim.

(A) *Engine installed in vehicle*

Performed either with open pipe or original system. 'A' weighted one-third octave spectra often recorded, or data processed to each relevant engine order.

- (i) Data derived from drive by (I.S.O.) trial records.
Note: There will be contamination by other coherent sources.
- (ii) Rolling road measurements obtained near exhaust pipe discharge.
Notes: (a) Pipe or system can be routed to minimize contamination.
(b) Narrow band spectral measurements possible.
- (iii) Vehicle mounted microphone near exhaust outlet.
Notes: (a) Contamination by wind noise, tyre noise etc.
(b) Representative warm up and operating conditions possible.
- (iv) Pipe wall mounted transducers, with digital signal capture and processing.
Note: Transducer cooling and calibration can be a problem.

(b) *Test bed measurements*

Advantages: Test conditions under close control with automated data capture and processing possible.

- (i) Microphone near exhaust outlet. (a) "open pipe or original system" (b) "new design validation" results may describe an insertion loss spectrum, or improvements in performance at the relevant engine orders.
Notes: (a) temperature gradients, etc., may not be representative
(b) a specific site environment is essential
(c) installation and operating costs may be relatively high.
- (ii) Pipe wall mounted pressure transducers—digital signal capture and processing.
Notes: (a) rapid and comprehensive data capture possible,
(b) characteristics of individual components can be quantified,
(c) with appropriate test bed automation, transient and steady state behaviour can be measured,
(d) initial system installation costs can be balanced against additional flexibility and reduced running time,
(e) fluctuating pressure amplitudes high—non-linear transducer response?
(f) changes in exhaust driving signal with modified exhaust system can be established,
(g) data may still not properly represent all actual operational conditions, e.g., temperature environment in system.

APPENDIX C: ASSESSMENT OF SOUND EMISSION FROM INTAKES AND EXHAUSTS

C.1. INTRODUCTION

A realistic quantitative prediction of source emission from intake or exhaust requires relevant and reliable descriptions both of the excitation and of the resulting wave energy transmission to the open termination. All intake and exhaust systems consist of a sequence of pipes connecting the silencer boxes, dust filters and other essential components that include various discontinuities either in cross-section area or wall impedance. Since any discontinuity both reflects and transmits wave energy, the wave motion throughout the system consists of positively and negatively travelling interfering waves. So long as the transverse dimensions remain a small fraction of the significant wavelengths, a valid approximation is that the associated fluid motion remains one-dimensional. Provided also that the waves propagate through the pipes without a significant change of shape, one can adopt the acoustic approximation and describe the wave motion by linear acoustic models in the frequency domain.

Since the emitted sound is normally described by its acoustic spectrum, descriptions of the wave motion in terms of the complex amplitudes of each spectral component of the fluctuating acoustic pressure p and particle velocity u , as they relate to plane acoustic wave motion, are relevant here. The corresponding complex amplitudes of each spectral component with wavenumber $k = 2\pi f/c$, or ω/c , are then given by p^+ for positively and p^- for negatively travelling waves. With plane acoustic waves, at each frequency the spectral component amplitudes are related by

$$p = p^+ + p^-, \quad \rho_0 c_0 u = p^+ - p^-, \quad (\text{C1}, 2)$$

where ρ_0 and c_0 are, respectively, the local ambient density and sound speed, while p , u , p^+ and p^- are all functions of position along the system. Equation (C1) is valid irrespective of the presence of a steady mean flow u_0 , while equation (C2) is similarly valid [3] so long as the viscothermal effects remain negligible.

One notes that waves propagate without change of shape (i.e., acoustically) only so long as their fluctuating pressure amplitude remains a small fraction of the ambient pressure. In manifolds in particular, the wave amplitude exceeds this limit by a substantial margin. However, in practice the distance between discontinuities remains too short for significant wave steepening to occur, so that wave propagation there may still be adequately described by the corresponding acoustic waves. One notes too that the valve/manifold combination represents a time varying system so that temporal descriptions of the wave motion are then appropriate. However, since the engine operations are cyclic the wave motion can be analysed in time and then Fourier transformed to provide its equivalent spectral description. Thus all discussions of wave propagation that follow here will be expressed in terms of the relevant spectral component amplitudes p and u or alternatively, the corresponding component wave amplitudes p^\pm and calculated one frequency at a time.

C.2. GENERAL MODELS OF ACOUSTIC PERFORMANCE

As described in section 2.2, compact spectral descriptions summarizing the acoustic behaviour of the system, or of each of its constituent elements, play an essential role in rational system design and optimization. At each frequency, acoustic plane wave transmission across an individual element or sequence of elements is illustrated in Figure A1. Here S represents the source of excitation for the element or sequence T , for which Z represents the acoustic impedance at its termination, with reflection coefficient $r = p_2^-/p_2^+$.

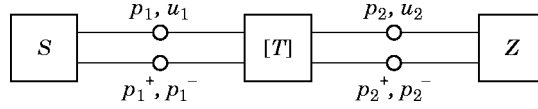


Figure A1. Plane wave acoustic transmission across elements.

At each frequency, the wave components p_1^\pm on the source side of T can be related to p_2^\pm on the load side by

$$p_1^+ = T_{11}p_2^+ + T_{12}p_2^-, \quad p_1^- = T_{21}p_1^+ T_{22}p_2^-, \quad (\text{C3a, b})$$

where T_{11} , T_{12} , T_{21} and T_{22} are the four elements of the scattering transmission matrix $[T]$ defining the transfer. The complex values of these four elements are functions of geometry, of the undisturbed values ρ_o and c_o , of the frequency of excitation, and of the mean flow Mach number M , but remain independent of the value of Z . Obviously equations (C1) and (C2) imply that the fluctuating acoustic pressure p_1 and velocity u_1 on the source side of T can be related to p_2 and u_2 on the load side in terms of the corresponding impedance transfer matrix $[t]$ by expressions analogous to equations (C3). The relative difficulty of measuring acoustic particle velocity u compared with measurements of p , combined with the restricted validity [3] of equation (C2), suggests that the scattering matrix $[T]$ provides a more robust description of the measured or predicted wave transfer than does the impedance matrix $[t]$.

Returning to Figure A1, we see that acoustic wave transmission across T can also be expressed in terms of the transmission coefficients

$$T_i = p_1^+ / p_2^+, \quad T_r = p_1^- / p_2^-, \quad (\text{C4a, b})$$

together with the reflection coefficient r where

$$r = p_2^- / p_2^+, \quad \text{or} \quad r = (\zeta - 1) / (\zeta + 1), \quad (\text{C5a, b})$$

and $\zeta = Z / \rho c$; also note that $p_1^- / p_1^+ = r T_r / T_i$. The transmission coefficients are related to the elements of the scattering matrix $[T]$ by

$$T_i = T_{11} + r T_{12}, \quad T_r = (T_{21} / r) + T_{22}, \quad (\text{C6a, b})$$

and it is evident that T_i and T_r are both functions of r and hence of Z as well as of the element's geometry, ρ , c , f and M . To evaluate the elements of $[T]$, one can easily show [8] that calculation or measurement of T_i and T_r with two different loads Za , Zb is necessary, unless $[T]$ possesses reciprocal properties. This cannot be true when mean flow is present, or when viscothermal or flow associated losses are significant, when evanescent waves are present and, as it turns out, when the element is not geometrically reciprocal. Thus transfer coefficients might be preferred to transfer matrix representations, despite the apparent convenience of the latter's independence of the load Z . Finally, one should note that both representations remain independent of the source of excitation, so long as it remains external to the element.

C.3. SINGLE PARAMETER DESCRIPTIONS

Intake and exhaust noise emission is often described in terms of the acoustic power radiated. A more useful description for system design is provided by the acoustic power W of each spectral component. Acoustic power is normally evaluated from measurements or calculations of the time averaged acoustic energy flux across unit area, expressed by the acoustic intensity I . In free space, for each spectral component, $I = \frac{1}{2} \text{Re}(p^* u)$ where $*$ indicates the complex conjugate, and p and u are the complex amplitudes (in this

representation the $\frac{1}{2}$ appears to correspond to time averaging of the real simple harmonic signals over a period). In the present context when a mean flow with Mach number u_o/c_o is invariably present, sound energy is also convected by the mean flow. Thus within the system and with plane acoustic waves, the spectral components of the acoustic energy flux per unit area are expressed [3] by

$$\rho_o c_o I = (1 + M)^2 |p^+|^2 - (1 - M)^2 |p^-|^2, \quad (C7)$$

where $|p^+|^2$ and $|p^-|^2$ are the squared moduli of p^+ and p^- .

Single parameter descriptions of system acoustic performance are common. Normally they define the acoustic attenuation of the system or element T , or of its transmission loss index TL , or insertion loss index IL , all expressed in decibels. The transmission loss of an acoustic element is usually defined as the difference in power flux *in free space* between that incident on and that transmitted across it and is then an invariant property of the element. With reference to the element T in Figure A1, after establishing anechoic conditions by setting $Z = \rho c$ or $r = 0$, then

$$TL = 10 \log_{10} [(S_1 I_1) / (S_2 I_2)], \quad (C8)$$

where the intensity or power flux may be found from equation (C7) and S_i is the cross-sectional area of the duct. This index neglects acoustic interaction with other system elements, so is hardly relevant for intake or exhaust design assessments.

The insertion loss is the measured change in power flux at a specified receiver, when the acoustic transmission path between it and the source is modified by the insertion of the element, provided that the impedances of both source and receiver remain invariant. If W_1 is the power at the receiver before the insertion of the element, and W_2 that measured or calculated afterwards, then the insertion loss index is defined by

$$IL = 10 \log_{10} (W_1 / W_2). \quad (C9)$$

In practice it is normally necessary to provide a reference duct system of known performance to measure or calculate W_1 and then repeat this procedure with the element or system of interest. This also implies that the source impedance should be known and invariant. Since the impedance presented at the source by the reference system will normally differ from that under test, due compensation to the results may be necessary to account for any corresponding changes to the source when its impedance is not effectively infinite.

A simple index of performance, which remains independent of an external source, but is dependent only on the acoustic characteristics of the system with its operating load Z , is the attenuation index AL expressed as

$$AL = 20 \log_{10} |T_i|, \quad (C10)$$

which can provide a convenient guide when the source impedance is unknown.

C.4. ACOUSTIC EXCITATION OF INTAKE OR EXHAUST SYSTEMS

The transfer of acoustic energy or sound power from the source to the system is strongly influenced by the acoustic impedance or load that the system presents to the source. The acoustic characteristics of both system and source are functions of the frequency so the discussion that follows here applies strictly to each spectral component although it also applies in general to all of them. The acoustic circuit corresponding to Figure A1 has been extended to include two representations of the source in Figure A2.

In the acoustic circuit of Figure A2(a) the source is now represented by one spectral component of fluctuating volume velocity with root mean square value V_s and associated

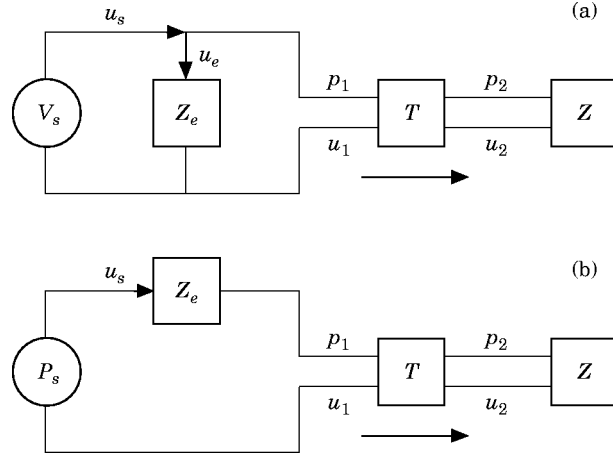


Figure A2. Acoustic representation of sources driving a system.

internal effective shunt impedance Z_e , while the corresponding system impedance at the source plane $Z_1 = p_1/u_1$. This representation corresponds say to fluctuating mass injection with an effective volume velocity $V_s = u_s S_s$. One notes that at the source plane the circuit model represents continuity of pressure with the source strength equated to a discontinuity of volume velocity. Thus this is equivalent to an acoustic monopole source in free space. The power output of this source is given by

$$W_r = \text{Re}\{p_1^* V_s\} = |V_s|^2 \text{Re}\{Z_1/(1 + Z_1/Z_e)\}/S_s, \quad (\text{C11a, b})$$

where the * represents the complex conjugate. Alternatively, when the source is associated with fluctuating aerodynamic forces, the circuit model of Figure A2(b) now represents the continuity of velocity u_s across the source plane with the source strength f_s equated to the discontinuity of pressure $(P_s - p_1)$ acting over area S_s , or $(P_s - p_1)S_s$. This is equivalent to an acoustic dipole source in free space. The power output is given by

$$W_r = \text{Re}\{f_s^* u_s\} = |f_s|^2 \text{Re}\{M_T\}, \quad (\text{C12a, b})$$

where the input ‘‘mobility’’ $M_T = u_s/f_s$, which also equals $1/Z_e S_s$ for the circuit in Figure A2(b). Analogous expressions can be derived for the sources of excitation by mixing noise associated with turbulent shear layers.

In practice, the source of excitation may include a combination of factors related to fluctuating mass, to fluctuating force and to flow turbulence. In all such cases the associated acoustic power delivered by the source to the system depends on the magnitude of the source impedance among other factors, while the acoustic emission from the open termination to the surroundings depends also on the efficiency [4] of power transfer through it. To illustrate the influence of the source and system impedance on such emissions, consider again the acoustic circuit of Figure A2(a). At the source plane the mass flux balance is given by

$$u_1 = u_s - p_1/Z_e, \quad \text{or} \quad Z_e u_s = p_1 + \rho_o c_o u_1 \zeta_e, \quad (\text{C13a, b})$$

where $\zeta_e = Z_e/\rho_o c_o$. Substituting for p_1 and $\rho_o c_o u_1$ in terms of the corresponding wave component amplitudes p_i^\pm from equations (C1, 2) into equation (C13b) and then making use of equations (C4a, b) and equation (C5b), one obtains

$$p_2^+ = Z_e u_s / [(1 + \zeta_e)T_i + (1 - \zeta_e)rT_r]. \quad (\text{C14})$$

If W_1 is the observed reference power and W_2 is the observed power with system T_2 , when a reference system T_1 is replaced by another system T_2 , provided the termination impedance Z and thus r remain constant and also similarly for Z_e and u_s , one finds that

$$(W_1/W_2) = |(p_2^+)_1 / (p_2^+)_2|^2, \quad (\text{C15})$$

which can be substituted for (W_1/W_2) in equation (C9) defining the insertion loss index. This is a common and convenient description of system performance.

C.5. SOUND PROPAGATION ALONG INTAKES AND EXHAUSTS

A physically realistic analysis of sound propagation along intakes and exhausts must begin with a complete analytical model of the associated fluid motion: that is, the equations of mass, linear momentum and energy transport, with those describing the relevant fluid properties and the geometrical and surface properties of the boundaries. Useful and sufficiently valid descriptions are obtained by assuming that the transfer processes remain isentropic and that the system is time invariant. With the acoustic approximation, sound propagation along the regular elements or pipes, can then be described by a linearized wave equation [3, 10] that may normally be Fourier transformed on the time t to describe the associated spectral characteristics. This procedure is described for plane wave propagation in Data sheet 1 (Data sheets 1–5 follow Appendix D).

Similar spectral descriptions of wave transfer across discontinuities may also be derived [3] by matching the associated fluid motion over appropriate surfaces on either side of the discontinuity, which together with any relevant fixed boundaries form a control volume. The equations expressing conservation of mass, energy and momentum are then expressed in integral form [3, 11]. The processes associated with the boundary conditions may include losses as well as the generation of non-propagating (evanescent) higher order modes, whose influence (normally reactive) must be included. One classical method of doing so it by the addition of an appropriate end correction [3] at such junctions. This general procedure is set out in Data sheet 2, with applications to open terminations, expansions with losses, and expansions and contractions with side branches, respectively, in Data sheets 3–5. These summarize part of the analysis set out in reference [3], so further details and other examples may be found there.

It has already been shown in equations (C6) that sound propagation along any acoustic component is always controlled, amongst other factors, by the impedance of its termination. Therefore it is logical to begin the acoustic analysis from its open termination, where the reflection coefficient (see Data sheet 3), or the associated impedance is simply calculated. This then defines the termination impedance of the system component nearest to the open end. Its input impedance then becomes the termination impedance for the next adjacent component and so on. Thus, in contrast to what one might expect the calculation of sound propagation along the system should begin at an open termination and proceed in sequence along the elements towards the source.

When the source characteristics are known, system acoustic performance can be expressed as insertion loss, as defined by equation (C9). If they have not been specified, which is usually the case, the relative acoustic performance may be expressed in terms of the system attenuation or equation (C10). Note that transmission loss, since it omits the influence of the termination, is not a relevant index here. Note too that such calculations rarely include the influence of flow noise generated by turbulence and separating flow elsewhere along the system. All acoustic performance predictions are subjected to uncertainties, to the extent that flow noise and the primary source characteristics remain undefined, in addition to any other deficiencies in the acoustic modelling.

APPENDIX D: LIST OF SYMBOLS AND ABBREVIATIONS

a	duct radius
c	speed of sound
d	pipe internal diameter
e_{ij}	end correction at area discontinuities
f	cyclic frequency
F	fluid boundary forces, f_s fluid force acting at source
h	specific enthalpy
I	acoustic intensity
k	wavenumber, ω/c
L	length, characteristic length
l	acoustic length
M	Mach number u_o/c_o
M_t	source mobility u_s/f_s
m	number of side branches
n	polytropic index
P	mechanical power
P_r	Prandtl number for acoustic medium
p	pressure
R_M	reflection coefficient modulus at Mach number M
r	pressure reflection coefficient, compression ratio
S	cross-section area
s	fluctuating entropy
T	system element
T_{ij}	elements of scattering matrix $[T]$
$T_i, T_r,$	forward and backward transmission coefficients
T_K, T_o	ambient absolute temperature
u	fluid velocity
V	control volume
V_s	source volume velocity
W	acoustic power
X	component length
x	axial displacement
Z	acoustic impedance p/u
α	visco-thermal factor
β	complex wavenumber
γ	ratio of the specific heats
δ	pressure perturbation associated with fluctuating entropy
ζ	specific impedance ratio $Z/\rho c$
η	efficiency
λ	acoustic wavelength
ν	kinematic viscosity
ρ	density
ω	radian frequency $2\pi f$

Subscripts

c	chamber, or cyclic
i	inner annulus
p	pipe
r	reference, averaged
o	ambient value, outer annulus
s	source, side branch

DATA SHEET 1: ACOUSTIC WAVE PROPAGATION ALONG FLOW DUCTS

A uniform pipe of length l , radius a , and mean flow at Mach number $M = u_o/c_o$ is illustrated in Figure A3. Dynamic equilibrium for fluctuations when $u(x, t) = u_o + u$, etc,

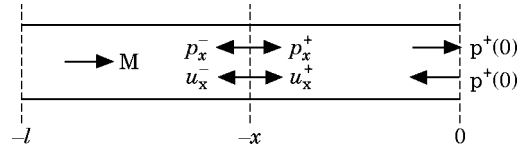


Figure A3. Uniform pipe with mean flow.

is expressed by

$$\rho_o[\partial/\partial t + u_o(\partial/\partial x)]u^+ = -\partial p^+/\partial x, \quad \rho_o[\partial/\partial t + u_o \partial/\partial x]u^- = -\partial p^-/\partial x.$$

This is satisfied at any x by

$$\begin{aligned} p^+(x, t) &= p^+(0) \exp i(\omega t - k^+ x), & u^+(x, t) &= u^+(0) \exp i(\omega t - k^+ x), \\ p^-(x, t) &= p^-(0) \exp i(\omega t + k^- x), & u^-(x, t) &= u^-(0) \exp i(\omega t + k^- x), \end{aligned}$$

where $k^+ = \omega/(c_o + u_o)$ and $k^- = \omega/(c_o - u_o)$. Also

$$\begin{aligned} p(x, t) &= p_x^+ + p_x^-, & \rho_o c_o u(x, t) &= p_x^+ - p_x^- \\ p(x, t) &= p^+(0) \exp i(Mk^*x) [\exp(-ik^*x) + r_o \exp(ik^*x)] \exp(i \omega t). \end{aligned}$$

where $k^* = (k^+ + k^-)/2 = (\omega/c_o)/(1 - M^2) = k/(1 - M^2)$. This represents a progressive and interfering wave motion, with node spacing defined by k^* .

$$\text{reflection coefficients: } r_o = p^-(0)/p^+(0), \quad r_x = p_x^-/p_x^+ = (\zeta x - 1)/(\zeta x + 1);$$

$$\begin{aligned} \text{impedances: } Z_o &= p(0)/u(0), & Z_x &= p_x/u_x = \rho_o c_o (p_x^+ + p_x^-)/(p_x^+ - p_x^-), \\ \zeta x &= Z_x/\rho_o c_o = (1 + r_x)/(1 - r_x); \end{aligned}$$

$$\text{transmission coefficients: } T_i = p_e^+/p_o^+, \quad T_r = p_e^-/p_o^-.$$

Note: with viscothermal wave attenuation, replace k by β , where $\beta = \omega/c_o + \alpha(1 - i)$, $\alpha = (1/ac_o)(\omega\nu/2)^{0.5} [1 + (\gamma - 1)Pr^{-0.5}]$, in which ν is the kinematic viscosity and Pr the Prandtl number. Then

$$p(x, t) = p_x^+ + p_x^-, \quad \rho_o c_o u(x, t) = d^+ p_x^+ - d_x^- p_x^-.$$

where

$$d^\pm = [k + \alpha(1 - i)]/[k \mp M\alpha(1 - i)].$$

DATA SHEET 2: WAVE COMPONENT TRANSFER AT DISCONTINUITIES

Given the geometry, M , T , p_2^+ , p_2^- , to find p_1^+ and p_1^- where mean variables are p_o , ρ_o , u_o etc, acoustic fluctuations, p , ρ , u , etc.

Follow a sequence of analytical steps.

(1) Identify and prescribe a relevant control volume V , with surface S .

(2) For the volume V set out the integral relations describing:

- (i) conservation of mass $\int_S \rho' u' dS = 0$ where $\rho' = \rho_o + \rho$, $u' = u_o + u$;
- (ii) conservation of energy $\int_S [h' + (u')^2/2] dS$; note; with isentropic processes $\rho = p/c_o^2$, enthalpy, $h' = h_o + p/\rho_o + T_o s$ and with fluctuating entropy, $s = (-1/\rho_o T_o) \delta/(\gamma - 1)$, $\rho = (p + \delta)/c_o^2$;

- (iii) momentum flux balance $\int_S [\rho'(u')^2 + p'] dS = \Sigma F = 0$, with fixed boundaries. Otherwise ΣF represents applied boundary forces.
- (3) Subtract the terms relating to the mean motion from (i), (ii) and (iii).
 - (4) Discard fluctuating terms of order higher than the first (acoustic approximation).
 - (5) Express fluctuating velocity u , density ρ and pressure p in terms of the equivalent progressive component wave amplitudes p^+ and p^- .
 - (6) Satisfy all relevant conditions at fixed boundaries. With rigid boundaries the component of u' normal to it will be zero. Either, (i) add appropriate set of evanescent higher order modes, or (ii) add appropriate end corrections, an effective procedure.
 - (7) The result will be a set of three equations expressing p_1^+ and p_1^- in terms of p_2^+ , p_2^- and δ . With isentropic processes, $\delta = 0$, so that (i) with either (ii) or (iii) are sufficient. Otherwise, eliminate δ first, to give two new equations in terms of p_2^+ and p_2^- alone.
 - (8) Solve for p_1^+ and p_1^- in terms of p_2^+ and p_2^- .
 - (9) Evaluate T_i , T_r , r_1 , for given $r_2 = p_2^- / p_2^+$.

DATA SHEET 3: PLANE WAVE REFLECTION AT AN OPEN UNFLANGED PIPE

The end of the pipe illustrated in Figure A4 is at $-l_o$, where $r = R_M \exp i\theta = -R_M \exp(-2ikl_M)$.

With zero mean flow and plane waves, pipe radius a , $0 < ka < 1.8$:

- (a) with $ka < 0.5$, $l_o/a = 0.6133 - 0.1168(ka)^2$; $0.5 < ka < 2$, $l_o/a = 0.6393 - 0.1104ka$;
- (b) $R_o = 1 + 0.01336 ka - 0.59079(ka)^2 + 0.33756(ka)^3 - 0.6432(ka)^4$.

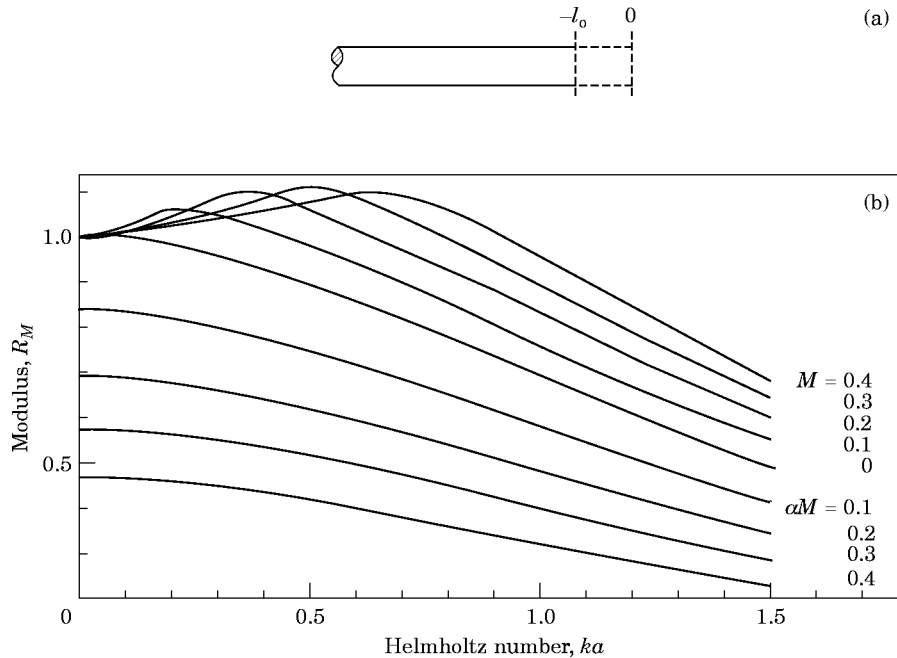
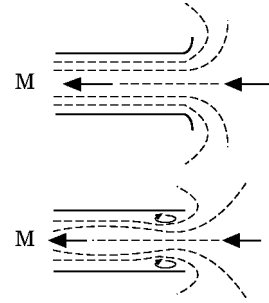


Figure A4. (a) An open unflanged pipe and end correction; (b) the modulus R_M of the reflection coefficient r , as a function of Helmholtz number ka , for inflow and for outflow when $R_M = R_o f(M)$.

With inflow at Mach number $\alpha M > 0$ (with smooth inflow $\alpha = 1$)

(a) $0 < M < 0.4$, $l_M = l_o [1 - M^2]$;

(b) $\begin{cases} 0 < M < 0.4 \\ 0 < \alpha M < 0.6 \end{cases} R_M = R_o [(1 - \alpha M)/(1 + \alpha M)]^{0.9}$.



With separating inflow, pressure loss coefficient K_p , $\alpha = 1 + (0.4K_p)^{0.5}$.

With outflow at $M > 0$,

(a) (i) $l_M = l_o$ or (ii) $l_M = l_o [1 - M^2]$, data inconclusive:

(b) $R_M = R_o f(M)$, see plots above.

A rather complex power series fit defining $f(M)$ exists.

Note that the evaluation of k and M requires the appropriate sound speed c_o corresponding to the local gas thermodynamic conditions.

DATA SHEET 4: TRANSFER CONDITIONS AT A FLOW DUCT EXPANSION

The control volume V is a plane at x , where Figure A5(b) shows mean velocity and Figure A5(c) acoustic pressure distribution. Note $u_r/u_o \sim 1$, $p/\bar{p} \sim 1$, where \bar{p} is the average acoustic pressure.

For the fluctuating quantities, the acoustic approximation gives

A. Conservation of mass: $\int_{S_1} (\rho_o u + u_o \rho)_1 dS_1 = \int_{S_2} (\rho_o u + u_o \rho)_2 dS_2$.

With wave component amplitudes, $M = u_o/c_o$, this becomes

$$[(1 + M)p_1^+ - (1 - M)p_1^-]S_1 = (S_2 + S_1 M)p_2^+ - (S_2 - S_1 M)p_2^- + \delta S_1 M$$

B. Conservation of energy: $\int_{S_1} (T_o s + p/\rho_o + u_o u)_1 dS_1 = \int_{S_2} (T_o s + p/\rho_o + u_o u)_2 dS_2$.

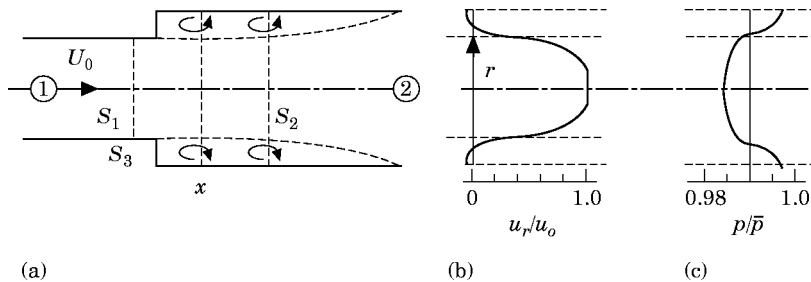


Figure A5. Transfer conditions at a flow duct expansion.

With wave component amplitudes, and ρ_o constant, this becomes

$$(1+M)p_1^+ + (1-M)p_1^- = (1+M)p_2^+ + (1-M)p_2^- - \delta/(\gamma-1).$$

C. *Momentum balance:* Since $V \rightarrow 0$, $M \sim \text{constant}$, $p/\bar{p} \sim 1.0$, and

$$[(\rho u_o^2 + 2\rho_o u_o u)_2 - (\rho u_o^2 + 2\rho_o u_o u)_1]S_1 = p_1 S_1 - p_2 S_2 + p_3 S_3.$$

With wave component amplitudes, since $(p_3^+ + p_3^-)S_3 = (p_2^+ + p_2^-)S_3$ this gives

$$[(1+M(M+2))p_1^+ + (1+M(M-2))p_1^-]S_1 = [M(M+2)p_2^+ + M(M-2)p_2^- + \delta M^2]S_1.$$

Note distribution of p_1 , p_2 , p_3 , across plane at x , from Figure A5(c). With isentropic processes, $\delta=0$, so that equation (A) with either (B) or (C) defines wave transfer neglecting evanescent waves. To include these by adopting end corrections, see Data sheet 5.

DATA SHEET 5: WAVE TRANSFER ACROSS EXPANSIONS AND CONTRACTIONS WITH SIDEBRANCHES

Figure A6 shows the geometry for calculation of component wave transfers across a discontinuity.

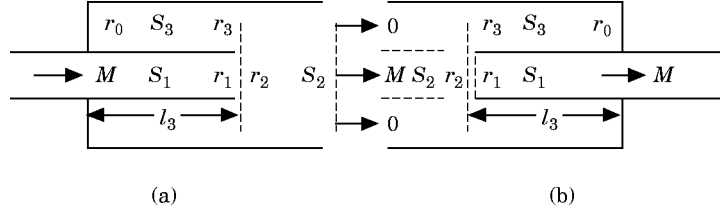


Figure A6. Geometry for calculation of component wave transfers across a discontinuity. (a) Expansion; (b) contraction.

With pipe radius a_1 , chamber hydraulic radius a_2 , one has the following steps.

Step 1: Calculate end correction $e_{21} = 0.63a_1 \{1 - \exp[-(1 - a_2/a_1)/1.5]\}$.

Step 2: Calculate side branch acoustic lengths, with physical length L at (a), $l_3 = [L_3 + e_{21}]$ at (b), $l_3 = -[L_3 + e_{21}]$.

Step 3: Calculate side branch reflection coefficients r_3 at (a), $r_3 = \exp(2ikl_3)/r_o$ at (b), $r_3 = r_o \exp(-2ikl_3)$.

Step 4: Evaluate $p_3 = p_3^+ + p_3^- = p_3^+(1 + r_3)$, $u_3 = p_3^+(1 - r_3)\rho_o c_o$.

Step 5: For control volume V , note that over V , $p_2 = p_3 = p_1$, and so for mass

$$\int_{S_1} (\rho_o u + u_o \rho)_1 dS_1 + \int_{S_3} \rho_o u_3 dS_3 = \int_{S_2} (\rho_o u + u_o \rho)_2 dS_2,$$

and for energy

$$\int_{S_1} (T_o s + p/\rho_o + u_o u)_1 dS_1 = \int_{S_2} (T_o s + p/\rho_o + u_o u)_2 dS_2 = \int_{S_3} (p_3/\rho_o) dS_3;$$

when processes are not isentropic include a momentum balance; see Data sheet 4.

Step 6: Express the three (or four) equations in terms of component waves,

$$p = p^+ + p^-, \quad \rho_o c_o u = p^+ - p^-, \quad \rho = (p^+ + p^-)/c_o^2 \text{ (if isentropic)}.$$

Step 7: Use $p_3^+(1 + r_3) = p_2^+ + p_2^-$ to eliminate $u_3 = (p_2^+ + p_2^-)(1 - r_3)/(1 + r_3)$.

Step 8: Solve for p_1^+ and p_1^- in terms of p_2^+ and p_2^- for (a), or *vice versa* for (b).

Step 9: Evaluate T_i , T_r etc, for known complex amplitudes p_2^+ and p_2^- ; see Figure A1.

Note: For a complete chamber calculate transfer from (b) to (a) using Data sheet 1. With intakes transfer will be from (a) to (b).